ARTICLE
Journal of Cellular Biochemistry 116:1693–1711 (2015)

Journal of Cellular Biochemistry

Gene Signatures of 1,25-Dihydroxyvitamin D_3 Exposure in Normal and Transformed Mammary Cells

Katrina M. Simmons,[1] Sarah G. Beaudin,[1] Carmen J. Narvaez,[1] and JoEllen Welsh[1,2]*

[1]*University at Albany Cancer Research Center, Biomedical Sciences, University at Albany, Rensselaer, New York 12144*

[2]*Cancer Research Center and the Departments of Biomedical Sciences and Environmental Health Sciences, SUNY Albany, Rensselaer, New York 12144*

ABSTRACT

To elucidate potential mediators of vitamin D receptor (VDR) action in breast cancer, we profiled the genomic effects of its ligand 1,25-dihydroxyvitamin D_3 (1,25D) in cells derived from normal mammary tissue and breast cancer. In non-transformed hTERT-HME cells, 483 1,25D responsive entities in 42 pathways were identified, whereas in MCF7 breast cancer cells, 249 1,25D responsive entities in 31 pathways were identified. Only 21 annotated genes were commonly altered by 1,25D in both MCF7 and hTERT-HME cells. Gene set enrichment analysis highlighted eight pathways (including senescence/autophagy, TGFβ signaling, endochondral ossification, and adipogenesis) commonly altered by 1,25D in hTERT-HME and MCF7 cells. Regulation of a subset of immune (*CD14, IL1RL1, MALL, CAMP, SEMA6D, TREM1, CSF1, IL33, TLR4*) and metabolic (*ITGB3, SLC1A1, G6PD, GLUL, HIF1A, KDR, BIRC3*) genes by 1,25D was confirmed in hTERT-HME cells and similar changes were observed in another comparable non-transformed mammary cell line (HME cells). The effects of 1,25D on these genes were retained in HME cells expressing SV40 large T antigen but were selectively abrogated in HME cells expressing SV40 + RAS and in MCF7 cells. Integration of the datasets from hTERT-HME and MCF7 cells with publically available RNA-SEQ data from 1,25D treated SKBR3 breast cancer cells enabled identification of an 11-gene signature representative of 1,25D exposure in all three breast-derived cell lines. Four of these 11 genes (*CYP24A1, CLMN, EFTUD1,* and *SERPINB1*) were also identified as 1,25D responsive in human breast tumor explants, suggesting that this gene signature may prove useful as a biomarker of vitamin D exposure in breast tissue. J. Cell. Biochem. 116: 1693–1711, 2015.

KEY WORDS: VITAMIN D RECEPTOR; BREAST CANCER; MAMMARY EPITHELIAL CELLS; GROWTH INHIBITION; GENOMIC PROFILING; MICROARRAY

Cholecalciferol (vitamin D3) is a seco-steroid that gives rise to 1α,25-dihydroxyvitamin D_3 (1,25D), the ligand for the nuclear vitamin D receptor (VDR). VDR is expressed in most tissues including the mammary gland [Berger et al., 1987; Zinser and Welsh, 2004] where it can heterodimerize with retinoid X receptors (RXR) to generate transcription complexes that induce and repress gene expression. Recent ChIP-Seq datasets generated from diverse human cell lines (osteoblasts, monocytes, lymphoblastoid cells, colorectal cancer cells, and hepatic stellate cells) indicate that liganded VDR binds 1,600–6,200 distinct genome regions depending on cell type, timing, and experimental protocol [Meyer et al., 2010, 2012; Heikkinen et al., 2011; Ding et al., 2013]. In these published datasets, the majority of VDR binding sites comprise direct-repeat 3 (DR3) sequences and co-localize with RXR binding and open chromatin but are not necessarily located in proximal promoter regions of regulated genes [Meyer et al., 2010, 2012; Heikkinen et al., 2011; Ding et al., 2013].

Sub-optimal vitamin D status is common in human populations and has been linked to a variety of chronic diseases including cancer. Epidemiologic studies largely support an inverse relationship between indices of vitamin D status (i.e., dietary intake, sun exposure, serum vitamin D metabolites) and breast cancer risk, progression, or mortality [Kim et al., 2014; Maalmi et al., 2014; Mohr et al., 2014; Vrieling et al., 2014]. Mechanistically, most breast tumors retain VDR gene expression although some studies suggest progressive loss of VDR expression and/or function as cancer

Katrina M. Simmons and Sarah G. Beaudin contributed equally to this work.

Grant sponsor: NIH; Grant numbers: R21CA166434, RC1CA144963, F31AT007276.

*Correspondence to: JoEllen Welsh, University at Albany Cancer Research Center, 1 Discovery Drive, Suite 304D, Rensselaer, NY 12144. E-mail: jwelsh@albany.edu

Manuscript Received: 2 December 2014; Manuscript Accepted: 6 February 2015

Accepted manuscript online in Wiley Online Library (wileyonlinelibrary.com): 3 March 2015

DOI 10.1002/jcb.25129 • © 2015 Wiley Periodicals, Inc.

progresses [Buras et al., 1994; Mittal et al., 2008; Lopes et al., 2010]. In VDR positive breast cancer cells, 1,25D exerts many anti-cancer actions including growth arrest, induction of apoptosis, and inhibition of migration/invasion [Laporta and Welsh, in press; Narvaez and Welsh, 2001; So et al., 2013]. Studies in mammary tumor cells derived from VDR null mice have demonstrated that the anti-cancer actions of 1,25D require functional VDR [Zinser et al., 2003] and scores of VDR regulated genes and proteins have been reported in various model systems of breast cancer [Swami et al., 2003; Byrne and Welsh, 2007; Goeman et al., 2014].

More recent mechanistic data supports the concept that 1,25D-VDR may signal in normal mammary cells to prevent or delay carcinogenesis [Kemmis et al., 2006; Rowling et al., 2006]. Non-tumorigenic human mammary epithelial (HME) cells express both VDR and CYP27B1, the enzyme that generates 1,25D from the circulating metabolite 25-hydroxyvitamin D (25D). In these cells, treatment with either 1,25D or 25D leads to growth arrest and induction of differentiation markers such as E-cadherin [Kemmis et al., 2006]. Similarly, in normal mouse mammary gland, 1,25D alters branching morphogenesis and inhibits hormone stimulated proliferation of the ductal epithelium in a VDR dependent manner [Zinser and Welsh, 2004]. The specific downstream targets that mediate the effects of 1,25D in normal mammary cells have yet to be defined, and the impact of transformation on VDR signaling has not been well-studied.

In the studies reported here, we used whole-genome profiling to compile a dataset of 1,25D regulated genes in cell lines derived from both normal mammary tissue and breast cancer. We subsequently explored the impact of transformation on several newly identified VDR targets related to innate immunity and cellular metabolism. Our data suggest that transformation is associated with reduced VDR expression which limits the induction of some, but not all, 1,25D gene targets. Despite these transformation-dependent changes in VDR signaling, integration of our gene lists with publically available array datasets enabled identification of an 11-gene signature representative of 1,25D exposure in both normal and transformed breast cells.

METHODS

CELL CULTURE

These studies employed non-transformed mammary epithelial cell lines as well as the breast cancer cell line MCF7. Two similar but unrelated lines of non-transformed mammary epithelial cells, both of which were derived from surgical resection of healthy female breast tissue, were used. Each was immortalized in independent labs through retroviral introduction of human telomerase reverse transcriptase (TERT). The hTERT-HME cell line was originally marketed by Clontech as the Infinity™ Human Mammary Epithelial Cell Line and is currently available from ATCC (CRL-4010). The other non-transformed mammary epithelial cell line (termed HME cells) was generated in a similar fashion by Dr. Robert Weinberg [Elenbaas et al., 2001] and was used for comparative purposes. Transformed derivatives of the Weinberg HME cell line were also studied, including the HME-LT cells (HME cells engineered for constitutive expression of the SV40 oncogene) and the HME-PR cells (constitutively expressing both SV40 and H*ras*^{V12}). These three cell lines constitute a well-studied model of mammary epithelial cell transformation [Elenbaas et al., 2001]. The hTERT-HME, HME, HME-LT, and HME-PR cell lines were maintained in serum-free M171 media containing mammary epithelial growth supplements (Life Technologies, Grand Island, NY). MCF7 human breast cancer cells, derived from a female invasive ductal carcinoma, were originally obtained from ATCC (Manassas, VA) and were cultured in α-Minimum Essential Media (α-MEM) supplemented with 5% fetal bovine serum (FBS). All cell lines were maintained in a 37°C and 5% CO_2 incubator and passaged every 3–4 days.

MICROARRAY PROFILING AND DATA ANALYSIS

RNA isolated from hTERT-HME or MCF7 cells (2–3 replicates) treated for 24 h with a pharmacologic dose of 100 nM 1,25-dihydroxyvitamin D_3 (1,25D, Sigma) or ethanol vehicle was hybridized to GeneChip® Human Gene ST 1.0 arrays (Affymetrix, Santa Clara, CA). The genomic datasets from the two cell lines were independently analyzed to identify 1,25D regulated genes using GeneSpring v 12.6 software (Agilent Technologies, Inc, Santa Clara, CA). Briefly, the baseline was transformed to the median of all samples and the data were filtered on expression (lower limit 20th percentile, upper limit 100th percentile). The filtered entities were statistically analyzed for the effect of 1,25D with a moderated *t*-test using Benjamini Hochberg FDR correction and a fold change limit of 1.5. The resulting lists (Supplementary Table S1) of 1,25D regulated genes ($P < 0.05$, fold change >1.5) from the two cell lines were subsequently subjected to Venn analysis on GeneSpring to identify overlap of the datasets. Pathway analysis was independently conducted for the entity lists derived from each cell line using pathways imported into GeneSpring from the Wiki Pathways portal (http://www.wikipathways.org/index.php/WikiPathways). Gene ontologies associated with the differentially expressed genes were identified with David Bioinformatics Resources v. 6.7 through GeneSpring.

To assess the degree of overlap of 1,25D responsive genes in these cell lines with other breast cancer model systems, comparative analysis was conducted with publically available datasets derived from 1,25D treated SKBR3 cells [Goeman et al., 2014] and breast tumor explants [Milani et al., 2013]. The SKBR3 dataset represents RNA-SEQ analysis of cells treated with 100 nM 1,25D for 6 h. The data were obtained from Supplementary Table S2 of the original paper [Goeman et al., 2014] which lists differentially expressed genes with at least 0.58 fold-change for the log2-transformed expression values filtered at the $P < 0.001$ level. The dataset of 1,25D regulated genes in breast tumor explants was obtained by microarray analysis of invasive breast cancer tissue incubated ex vivo with 100 nM 1,25D for 24 h as described by Milani et al. [Milani et al., 2013]. Genes with a fold change >1.5 (control vs. 1,25D-treated) with significance at the $P < 0.05$ level as assessed by repeated measures ANOVA were included in the comparative analyses. The raw data is available in GEO (Gene Expression Omnibus) Datasets under accession no. GSE27220.

INDEPENDENT VALIDATION OF GENE EXPRESSION

A subset of candidates identified by the microarray profiling as 1,25D-regulated genes in hTERT-HME and MCF7 cells was further assessed by qPCR in independent samples. For these assays, 10^6 cells (hTERT-HME, HME, HME-LT, HME-PR or MCF7) in 100 mm dishes were treated 24–48 h after plating with 100 nM 1,25D or ethanol vehicle for 24 h. All data are representative of 3–4 independent RNA isolations. RNA was isolated with the Qiagen RNeasy kit (Qiagen, Valencia, CA) and analyzed for concentration and purity on a Nanodrop 1000 Spectrophotometer. cDNA was prepared using TaqMan Reverse Transcriptase Reagents (Life Technologies, Grand Island, NY) and analyzed in duplicate using SYBR Green PCR Master Mix (ABgene-Thermo Scientific, Pittsburgh, PA) on an ABI Prism 7900HT Sequence Detection System (Applied Biosystems, Foster City, CA). Primer sequences were obtained from Origene and are listed in Supplementary Table S2. Data were calculated by the ΔΔCt method and normalized against 18S expression. When one cell type was analyzed, values for 1,25D treated cells were expressed relative to values obtained for vehicle treated cells. When multiple cell types were compared, data were expressed relative to one of the cell lines (i.e., HME for the transformed derivatives or MCF7 for the comparison to hTERT-HME cells) in order to better visualize differences in basal gene expression among the cell lines. Statistical analysis was conducted with GraphPad Prism software (La Jolla, CA) using a one-tailed, unpaired *t*-test (with Welch's correction when appropriate), one-way ANOVA or two-way ANOVA to test for differences in responsiveness to 1,25D among cell lines. For all data, *P*-values less than 0.05 were considered significant.

RESULTS

MICROARRAY PROFILING OF 1,25D-TREATED hTERT-HME CELLS

To identify targets of vitamin D signaling in non-transformed mammary epithelial cells, genomic profiles were examined in hTERT-HME cells treated for 24 h with 100 nM 1,25D. We identified 483 entities that were significantly ($P < 0.05$) altered >1.5 fold in response to 1,25D (319 up-regulated/164 down-regulated). Table I lists the top 20 up-regulated genes, which included *CYP24A1*, *CD14*, *ITGB3*, and *BMP6*. Table II lists the top 20 down-regulated genes, which included *KDR*, *BIRC3*, *RGS2*, and *GLUL*. The full list of annotated genes, with fold change in response to 1,25D treatment and *P* values, is available as Supplementary Table S1. Many of the genes in this dataset, including *CD14*, *IGFBP3*, *GRK5*, *BMP6* and *TGFB2* have been frequently reported as 1,25D responsive [Swami et al., 2003; Lee et al., 2006; Fleet et al., 2012].

Using WIKI pathways within the Genespring program we identified 42 pathways that were significantly ($P < 0.05$) enriched in this 1,25D-regulated dataset including senescence and autophagy, cell cycle checkpoints, and TGFβ signaling (Table III). Regulation of these pathways by 1,25D is not surprising since longer term incubation of hTERT-HME cultures with 100 nM 1,25D induces growth inhibition [Kemmis et al., 2006] and TGFβ is known to inhibit mammary epithelial cell growth [Zugmaier and Lippman, 1990]. Also consistent with a tumor suppressive effect of 1,25D, gene enrichment was noted for pathways related to oxidative stress, Nrf2 signaling and cell adhesion. 1,25D treatment also enriched for genes in pathways related to distinct differentiated phenotypes (adipogenesis, angiogenesis, ossification, and osteoclasts) as well as immune responses and cellular metabolism. The biological gene ontology (GO) terms altered by 1,25D in hTERT-HME cells (Supplementary Table S3) included wounding and inflammatory response, nutrient and vitamin response and cell migration and proliferation, each of which had >10 matching entities. Molecular GO terms altered by 1,25D included steroid dehydrogenase and oxidoreductase activity, growth factor and enzyme binding and enzyme inhibitor activity (Supplementary Table S4).

CONFIRMATION OF METABOLIC AND IMMUNE GENE REGULATION BY 1,25D IN hTERT-HME CELLS

We were particularly interested in the effects of 1,25D on metabolic (i.e., pentose phosphate pathway) and immune (i.e., Toll-like receptor signaling, cytokines, and inflammation) pathways as these have not previously been linked to VDR signaling in normal mammary cells yet are highly relevant to carcinogenesis. In addition to *CYP24A1*, seven immune response genes (*CD14*, *IL1RL1*, *MALL*, *TREM1*, *SEMA6D*, *CD274*, and *CSF1)* and eight genes related to cellular metabolism and hypoxia (*ITGB3*, *SLC1A1*, *IGFBP3*, *G6PD*, *KDR*, *BIRC3*, and *GLUL)* were altered >3 fold by 1,25D (Tables IV and V). We used qPCR to determine the expression of a subset of these candidate genes in the hTERT-HME cells under the same conditions (100 nM 1,25D treatment for 24 h). As shown in Figure 1, 10 of the 12 immune related genes were confirmed as 1,25D responsive by qPCR in these cells. *CD14*, *IL1RL1*, *MALL*, and *TREM1* were increased >50 fold whereas *CAMP* and *SEMA6D* were increased >10 fold in 1,25D-treated cells. *IL1RN* was confirmed as a 1,25D repressed gene. In contrast, *IL1B* expression was significantly reduced (rather than up-regulated) by 1,25D treatment, and neither *CD274 or IL8* were reproducibly altered by 1,25D.

We chose an additional eleven gene products related to cellular metabolism, hypoxia and growth factor signaling for qPCR analysis (Fig. 2). We first confirmed our previous finding [Beaudin et al., 2014] that the canonical VDR target gene *CYP24A1* which encodes a cytochrome P450 enzyme that metabolizes 1,25D, is highly induced (>5,000 fold) by 1,25D in this cell line (data not shown). Of the ten other genes examined, seven were validated as 1,25D responsive (four up-regulated and three down-regulated). The most highly up-regulated genes in this category (*ITGB3*, *SLC1A1*, and *G6PD*) were 5–20 fold higher in 1,25D-treated cells than control cells. Expression of *HIF1A*, *IDH2*, and *PGD* genes was elevated 1.5–2 fold in 1,25D-treated compared to control cells, but only *HIF1A* was statistically significant. Three genes that were identified as down-regulated by 1,25D through microarray profiling (*BIRC3*, *GLUL*, and *KDR*) were confirmed by qPCR to be reduced 70–90% in treated cells. Although found as an up-regulated gene in the array dataset, *IGFBP3* was not confirmed by PCR as differentially expressed in 1,25D-treated hTERT-HME cells (data not shown).

EFFECT OF TRANSFORMATION ON 1,25D MEDIATED GENE REGULATION

To determine whether genomic regulation by 1,25D in hTERT-HME cells was recapitulated in an independently derived immortalized

TABLE I. Top 20 Up-Regulated Genes in hTERT-HME Cells Exposed to 100 nM 1,25D for 24 h

Gene symbol	Gene description	Fold change[1]	Corrected *P*-value[2]
CYP24A1	Cytochrome P450, Family 24A1	181.37	3.65E-10
CD14	CD 14 Molecule	72.04	3.48E-08
ITGB3	Integrin, Beta 3	13.88	9.27E-09
BMP6	Bone Morphogenetic Protein 6	13.34	3.48E-08
DHRS9	Dehydrogenase/Reductase Member 9	9.88	1.17E-08
IL1RL1	Interleukin 1 Receptor-Like 1	8.02	1.07E-07
MALL	Mai, T-Cell Differentiation Protein-Like	7.62	3.49E-08
FAM20C	Family With Sequence Similarity 20. Member C	7.39	1.05E-07
SLC1A1	Solute Carrier Family 1 (Neuronal/Epithelial High Affinity Glutamate Transporter. System Xag), Member 1	7.13	4.81E-07
PDE2A	Phosphodiesterase 2A, Cgmp-Stimulated	7.07	3.26E-08
SEMA3B	Semaphorin 3B	6.69	4.81E-07
TREM1	Triggering Receptor Expressed On Myeloid Cells 1	6.52	7.84E-08
SEMA6D	Semaphorin 6D	6.47	2.86E-07
ID2	Inhibitor Of DNA Binding 2	6.41	2.17E-06
CASP14	Caspase 14	6.30	6.24E-07
THBD	Thrombomodulin	5.45	2.24E-06
APBB3	Amyloid Beta Precursor Protein-Binding B3	5.01	1.83E-06
AKAP12	A Kinase Anchor Protein 12	4.88	4.38E-07
ID1	Inhibitor Of DNA Binding 1	4.86	4.51E-06
CALML3	Calmodulin-Like 3	4.33	4.15E-07

[1]Fold change in hTERT-HME cells treated with 100 nM 1,25D relative to ethanol vehicle was calculated from microarray data with Gene Spring.
[2]*P*-values were generated by moderated *t*-test with Benjamini Hochberg correction.

mammary epithelial cell line, we utilized the HME cell line generated by the Weinberg lab [Elenbaas et al., 2001]. An advantage of this cell line is the availability of isogenic derivatives expressing SV40 (HME-LT cells) or SV40 plus oncogenic RAS (HME-PR cells) which allowed us to examine the effect of transformation on 1,25D signaling. The effect of 1,25D on *VDR* expression and a subset of 1,25D target genes identified in the hTERT-HME cells was evaluated. In the immortalized but non-transformed HME cells, 1,25D down-regulated *VDR* expression while increasing *CYP24A1* >900 fold (Fig. 3). Comparison of the first two bars of each graph in Figures 4 and 5 (which represent data from control and 1,25D treated HME cells) with the hTERT data (Figs. 1 and 2) indicates that all of the genes selected for follow-up based on the hTERT-HME array dataset showed the same pattern of response to 1,25D in the HME cells (i.e., *CD14*, *IL1RL1*, *IL33*, *BMP6*, *ITGB3*, *HIF1A*, and *SLC1A1* were up-regulated whereas *BIRC3*, *GLUL*, and *KDR* were down-regulated). These strong similarities in the genomic responses to 1,25D were expected based on a recent report by our group in which 1,25D regulation of a small subset of these genes was compared in these two cell lines [Beaudin et al., 2014].

In previous studies, we observed that *VDR* is down-regulated as a function of transformation [Kemmis and Welsh, 2008] and others have observed inverse correlations between *VDR* expression and clinical stage in human breast tumors [Lopes et al., 2010]. Thus, it

TABLE II. Top 20 Down-Regulated Genes in hTERT-HME Cells Exposed to 100 nM 1,25D for 24 h

Gene symbol	Gene description	Fold change[1]	Corrected *P*-value[2]
KDR	Kinase Insert Domain Receptor	−6.63	3.92E-07
BIRC3	Baculoviral IAP Repeat-Containing 3	−5.14	2.70E-06
RGS2	Regulator of G-Protein Signaling 2,24 kDa	−5.01	3.92E-07
GLUL	Glutamate-Ammonia Ligase	−4.06	2.19E-07
GLUL	Glutamate-Ammonia Ligase	−3.82	2.86E-07
LAPTM5	Lysosomal Protein Transmembrane 5	−3.07	1.33E-05
SLC7A2	Solute Carrier Family 7 (Cationic Amino Acid Transporter, Y + System), Member 2	−2.95	2.70E-06
F2RL2	Coagulation Factor II Receptor-Like 2	−2.80	8.98E-06
S100A8	SI00 Calcium Binding Protein A8	−2.78	2.00E-05
AGR2	Anterior Gradient Homolog 2	−2.72	3.15E-05
SPRR1B	Small Proline-Rich Protein IB	-2.70	5.30E-05
PLAU	Plasminogen Activator, Urokinase	−2.63	1.55E-06
SERPINB2	Serpin Peptidase Inhibitor, Clade B, Member 2	−2.61	8.31E-06
FOSB	FBJ Murine Osteosarcoma Viral Oncogene Homolog B	−2.59	1.22E-05
APOD	Apolipoprotein D	−2.49	7.55E-06
SCNN1G	Sodium Channel, Nonvoltage-Gated 1, Gamma	−2.40	4.95E-06
TRIM29	Tripartite Motif-Containing 29	−2.35	4.51E-06
SLITRK6	SLIT and NTRK-Like Family, Member 6	−2.30	5.44E-05
ABCG1	ATP-Binding Cassette, Sub-Family G, Member 1	−2.21	8.22E-06
REPS2	RALBP1 Associated Eps Domain Containing 2	−2.11	4.87E-05

[1]Fold change in hTERT-HME cells treated with 100 nM 1,25D relative to ethanol vehicle was calculated from microarray data with Gene Spring.
[2]*P*-values were generated by moderated *t*-test with Benjamini Hochberg correction.

TABLE III. Pathway Analysis of Differentially Expressed Genes in hTERT-HME Cells Exposed to 100 nM 1,25D for 24 h

Pathway	*P*-value[1]	Matched entities[2]	Number of pathway entities[3]
Senescence and Autophagy	1.48E-04	9	106
Oxidative Stress	2.32E-04	5	30
Adipogenesis	2.56E-04	10	131
Endochondral Ossification	2.57E-04	7	64
Complement and Coagulation Cascades	4.28E-04	6	64
TGF Beta Signaling Pathway	6.52E-04	6	55
Prolactin Signaling Pathway	7.40E-04	7	76
Serotonin Transporter Activity	1.11E-03	3	11
Angiogenesis	1.11E-03	3	24
Transcriptional activation by NRF2	2.34E-03	3	14
Osteoclast Signaling	2.34E-03	3	16
Alpha 6 Beta 4 signaling pathway	3.05E-03	4	33
Arrhythmogenic Right Ventricular Cardiomyopathy	3.36E-03	6	78
ID signaling pathway	3.50E-03	3	16
Toll-like receptor signaling pathway	4.05E-03	7	102
Regulation of toll-like receptor signaling pathway	4.05E-03	7	150
Pentose Phosphate Pathway	7.60E-03	2	7
Dissolution of Fibrin Clot	1.00E-02	2	8
Cytokines and Inflammatory Response	1.00E-02	3	30
Myometrial Relaxation and Contraction Pathways	1.18E-02	8	156
Integrin alphallb beta3 signaling	1.27E-02	2	12
Regulation of IGF Activity by IGFBPs	1.57E-02	2	10
Wnt Signaling Pathway	1.78E-02	4	51
Vitamin D Metabolism	1.89E-02	2	11
Interferon gamma signaling	1.89E-02	2	13
Interferon type I	2.16E-02	4	54
RANKL-RANK Signaling Pathway	2.29E-02	4	55
Osteopontin Signaling	2.61E-02	2	13
Nuclear Receptors in Lipid Metabolism and Toxicity	2.67E-02	3	35
Fluoropyrimidine Activity	2.67E-02	3	33
Focal Adhesion	2.96E-02	8	188
Corticotropin-releasing hormone	3.12E-02	5	90
Leptin signaling pathway	3.20E-02	4	61
Cell Cycle Checkpoints	3.42E-02	2	16
Oncostatin M Signaling Pathway	3.55E-02	4	65
Signaling by VEGF	3.90E-02	1	3
EGF-EGFR Signaling Pathway	4.04E-02	7	162
Circadian Clock	4.32E-02	2	17
Integrated Pancreatic Cancer Pathway	4.37E-02	3	200
Integrin-mediated Cell Adhesion	4.59E-02	5	99
Semaphorin interactions	4.80E-02	2	20
MAPK Signaling Pathway	4.89E-02	7	168

[1]*P*-values were calculated for pathway enrichment with Wiki Pathways Beta.
[2]Number of matched entities from the microarray dataset.
[3]Total number of entities for each pathway.

TABLE IV. Immune Response Genes Up-Regulated by 1,25D in hTERT-HME Cells

Gene symbol	Gene description	Fold Change[1]	Corrected *P*-value[2]
CD14	CD 14 Molecule	72.04	3.48E-08
IL1RL1	Interleukin 1 Receptor-Like 1	8.02	1.07E-07
MALL	Mai. T-cell Differentiation Protein-Like	7.62	3.49E-08
TREM1	Triggering Receptor Expressed on Myeloid Cells 1	6.52	7.84E-08
SEMA6D	Semaphorin 6D	6.47	2.86E-07
CD274	CD274 Molecule	3.61	3.49E-06
CSF1	Colony Stimulating Factor 1	3.33	6.24E-07
IL8	Interleukin 8	2.53	8.98E-06
CAMP	Cathelicidin Antimicrobial Peptide	2.40	9.95E-06
TLR4	Toll-Like Receptor 4	2.34	3.39E-04
IL1B	Interleukin 1, Beta	1.82	5.23E-05
IL33	Interleukin 33	1.58	9.72E-04

[1]Fold change in hTERT-HME cells treated with 100 nM 1,25D relative to ethanol vehicle was calculated from microarray data with Gene Spring.
[2]*P*-values were generated by moderated *t*-test with Benjamini Hochberg correction.

TABLE V. Genes Related to Cellular Metabolism and Hypoxia Altered by 1,25D in hTERT-HME Cells

Gene symbol	Gene description	Fold Change[1]	Corrected *P*-value[2]
ITGB3	Integrin, Beta 3	13.88	9.27E-09
SLC1A1	Solute Carrier Family 1A1	7.13	4.81E-07
IGFBP3	Insulin-Like Growth Factor Binding Protein 3	3.79	3.94E-07
G6PD	Glucose-6-Phosphate Dehydrogenase	3.73	2.13E-07
PGD	Phosphogluconate Dehydrogenase	1.74	1.49E-04
IDH2	Isocitrate Dehydrogenase 2	1.55	1.67E-04
HIF1A	Hypoxia Inducible Factor 1, Alpha	1.54	2.13E-04
GLUL	Glutamate-Ammonia Ligase	−4.06	2.19E-07
BIRC3	Baculoviral lap Repeat-Containing 3	−5.14	2.70E-06
KDR	Kinase Insert Domain Receptor	−6.63	3.92E-07

[1]Fold change in hTERT-HME cells treated with 100 nM 1,25D relative to ethanol vehicle was calculated from microarray data with Gene Spring.
[2]*P*-values were generated by moderated *t*-test with Benjamini Hochberg correction.

was of interest to compare the regulation of these newly identified VDR targets by 1,25D in the parental HME cells and their progressively transformed derivatives. In the present study we confirmed our previous data [Kemmis and Welsh, 2008] that *VDR* is reduced about 15% in cells expressing SV40 (HME-LT cells) and almost 80% in cells expressing both SV40 and RAS (HME-PR cells) compared to HME cells. (Fig. 3A). The repression of *VDR* by 1,25D that occurred in HME cells was observed in HME-LT cells but not in HME-PR cells (two-way ANOVA indicated a significant difference in response to 1,25D in HME-PR cells). However, despite the reduction in *VDR* expression, 1,25D robustly induced the direct VDR target gene *CYP24A1* in all three HME derivative cell lines (1,000–1,500 fold increase over vehicle-treated control cells; Fig. 3B). Two-way ANOVA indicated that induction of *CYP24A1* was significantly greater in the HME-PR cells than in the HME or HME-LT cells. These data indicate that sufficient receptor is retained even in HME-PR cells for strong transcriptional activation of VDREs in the presence of ligand. With respect to the newly identified gene targets, we found that introduction of SV40 into HME cells minimally impacted cellular responsiveness to 1,25D (Fig. 4). Thus, *CD14*, *IL1RL1*, *BMP6*, *ITGB3*, *IL33*, *HIF1A,* and *SLC1A1* were similarly induced and *BIRC3*, *GLUL* and *KDR* were similarly repressed by 1,25D in HME and HME-LT cells. In contrast, introduction of oncogenic RAS selectively altered the genomic effects of 1,25D. Despite reduced *VDR* expression and RAS activation, two immune response genes (*CD14* and *IL33*) were induced by 1,25D to the same magnitude in the HME-PR cells as in the HME and HME-LT cells. Four other genes (*IL1RL1*, *BMP6*, *ITGB3*, and *SLC1A1*) were significantly up-regulated by 1,25D in the HME-PR cells but the magnitude was less than that in HME or HME-LT cells. In contrast, the expression of *HIF1A* (which was up-regulated by 1,25D in HME and HME-LT cells) and *BIRC3*, *GLUL,* and *KDR* (which were down-regulated by 1,25D in HME and HME-LT cells) were unchanged in response to 1,25D in the HME-PR cells. Collectively, these data suggest that RAS transformation elicits complex effects on VDR signaling leading to deregulation of a subset of 1,25D target genes.

GENOMIC EFFECTS OF 1,25D IN MCF7 BREAST CANCER CELLS

Given the altered responses to 1,25D in RAS transformed HME derivatives, we further explored the effects of 1,25D on several of these target genes in the human breast cancer cell line MCF7. This VDR positive cell line has been extensively used for study of the anti-cancer effects of 1,25D but does not express oncogenic RAS. We used PCR to assess the effect of 1,25D (100 nM, 24 h) on expression of *CYP24A1* and several of the target genes identified in the hTERT-HME array dataset. As shown in Figure 6, the VDR in MCF7 cells is highly capable of inducing *CYP24A1* expression in response to 1,25D (>6,000 fold over control values). Of the eight other genes examined in MCF7 cells, two (*CD14* and *KDR*) were regulated in a similar manner to that observed in hTERT-HME and HME cells, but the magnitude of the effect was substantially less. 1,25D had no effect on expression of *IL1RL1, SLC1A1, GLUL* or *BIRC3*, and decreased (rather than increased) expression of *BMP6* and *ITGB3* in MCF7 cells. This data indicated that only three (*CYP24A1*, *CD14,* and *KDR*) of the nine genes examined were similarly regulated by 1,25D in MCF7 and hTERT-HME cells. Others were either unaffected by 1,25D or regulated in an opposite direction in the two cell lines.

Collectively, these data suggested that the genomic effects of 1,25D are quite distinct in cells derived from normal breast (hTERT-HME and HME) and cells derived from breast cancer (MCF7). Although 1,25D is known to induce growth arrest and apoptosis in MCF7 cells [Simboli-Campbell et al., 1996, 1997], whole-genome profiles of 1,25D treatment have not been published for this cell line. To comprehensively compare the VDR regulated transcriptome between these two cell types, we conducted microarray profiling of 1,25D treated MCF7 cells using the same analysis platform as for hTERT-HME cells. In response to 24 h treatment with 100 nM 1,25D, 249 entities were significantly ($P < 0.05$) altered >1.5 fold in MCF7 cells (153 up-regulated/96 down-regulated). Table VI lists the top 20 up-regulated genes, all of which were induced >2.5 fold including *CYP24A1*, *KLK6*, *TRPV6, CP,* and *MERTK*. With respect to down-regulation (Table VII), only four of the top 20 genes (*PMP22*, *CTGF*, *CLDN1,* and *ILIR1*) were reduced >2 fold by 1,25D in MCF7 cells.

Pathway analysis of the MCF7 data conducted at the same significance level ($P < 0.05$) as for the hTERT-HME dataset indicated enrichment of genes in 31 pathways after 1,25D treatment (Table VIII). Eight of these pathways (senescence and autophagy, TGFβ signaling, endochondral ossification, adipogenesis, nuclear receptors in lipid metabolism/toxicity, oncostatin M signaling, integrated pancreatic cancer pathway, and integrin mediated cell adhesion) were common to those enriched in the 1,25D-treated hTERT-HME

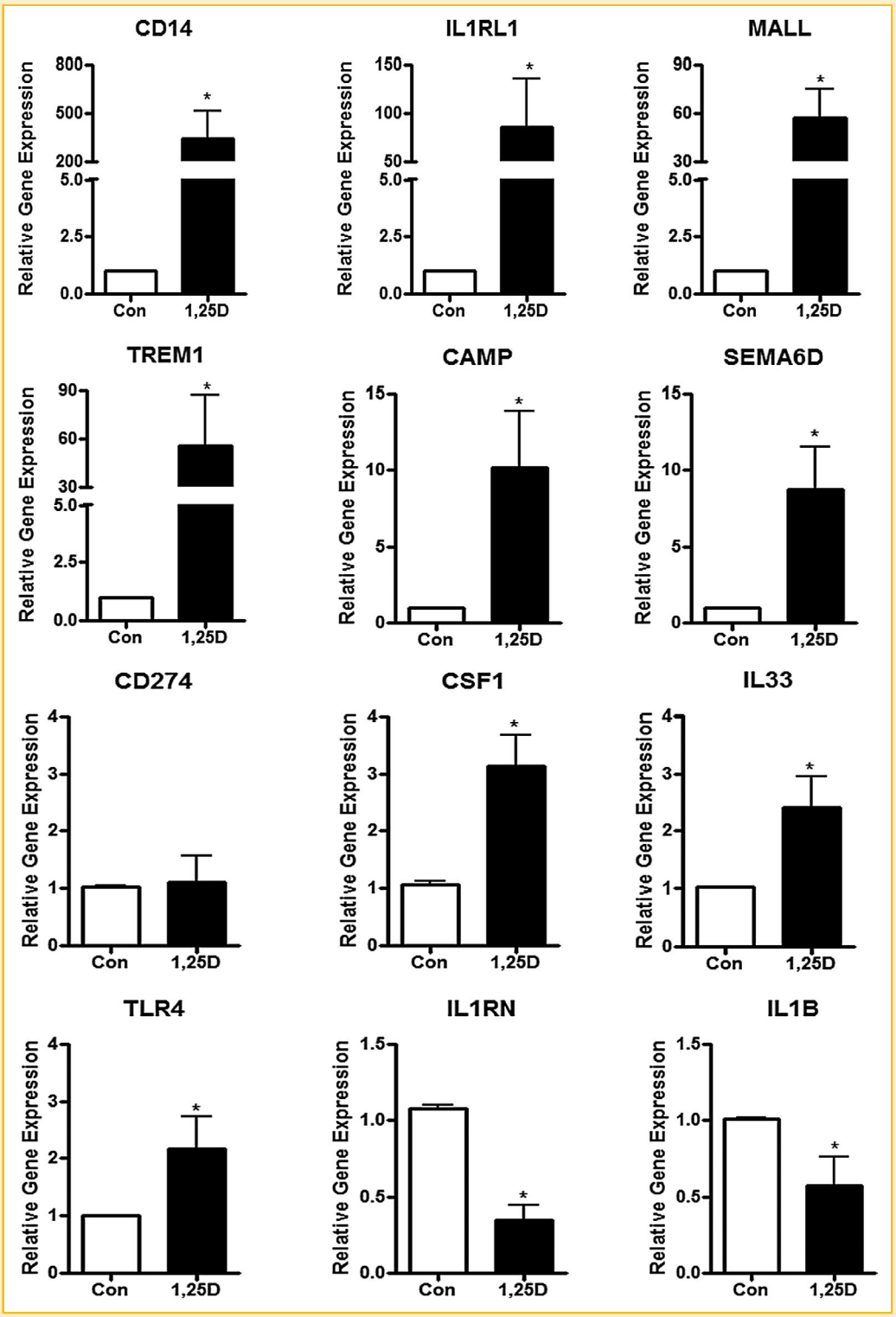

Fig. 1. Quantitative PCR analysis of selected immune gene expression in 1,25D treated hTERT-HME cells. hTERT-HME cells were treated with 100 nM 1,25D or ethanol vehicle (Con) for 24 h. RNA was isolated and real-time quantitative PCR was conducted for *CD14, IL1RL1, MALL, TREM1, CAMP, SEMA6D, CSF1, IL33, TLR4,* and *IL1RN*. The data were normalized against 18S and expressed as relative gene expression with values for control cells which were set to 1. Each bar represents mean ± standard deviation of at least three independent biological repeats analyzed in duplicate. *P-value <0.05 as assessed by one-tailed, unpaired t-test with Welch's correction.

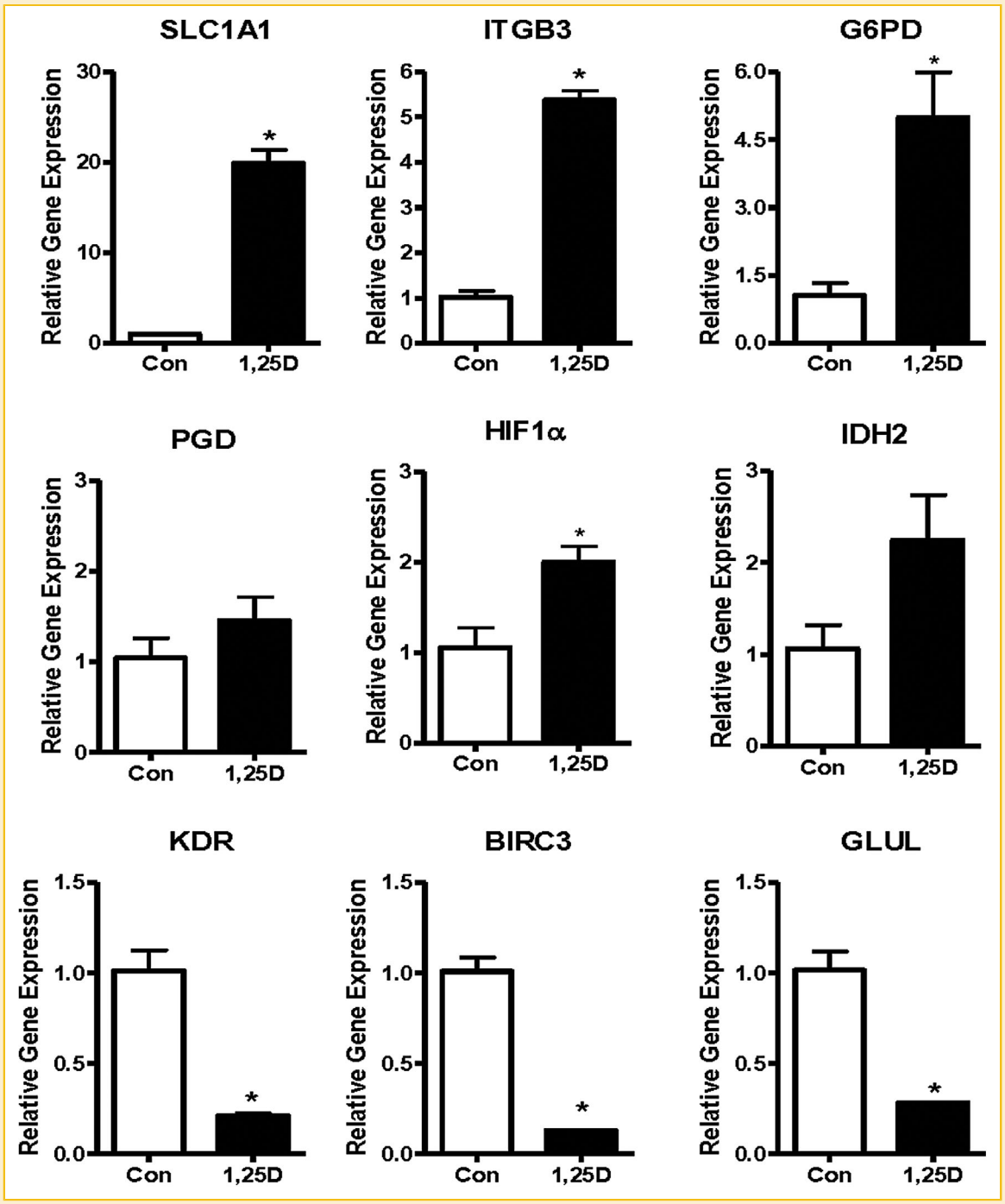

Fig. 2. Quantitative PCR analysis of genes involved in cellular metabolism and hypoxia in 1,25D treated hTERT-HME cells. hTERT-HME cells were treated with 100 nM 1,25D or ethanol vehicle (Con) for 24 h. RNA was isolated and real-time quantitative PCR was conducted for *SLC1A1*, *ITGB3*, *G6PD*, *PGD*, *HIF1A*, IDH2, KDR, BIRC3, and GLUL. The data were normalized against 18S and expressed relative to values for control cells which were set to 1. Each bar represents mean ± standard deviation of at least three independent samples analyzed in duplicate. *P-value <0.05 as assessed by one-tailed, unpaired t-test.

cells. High scoring cancer-relevant pathways in the 1,25D-treated MCF7 cell dataset that were not enriched in the hTERT-HME dataset included Phase I metabolism, apoptosis modulation and signaling, estrogen/tamoxifen metabolism and ATM signaling. Gene ontology (GO) analysis identified 1,25D responsive biological processes common to both the MCF7 and hTERT-HME datasets including response to vitamins, nutrients and wounding, and regulation of cell proliferation. Additional lists of biological and molecular GO terms altered by 1,25D in MCF7 cells are reported in Supplementary Tables S5 and S6.

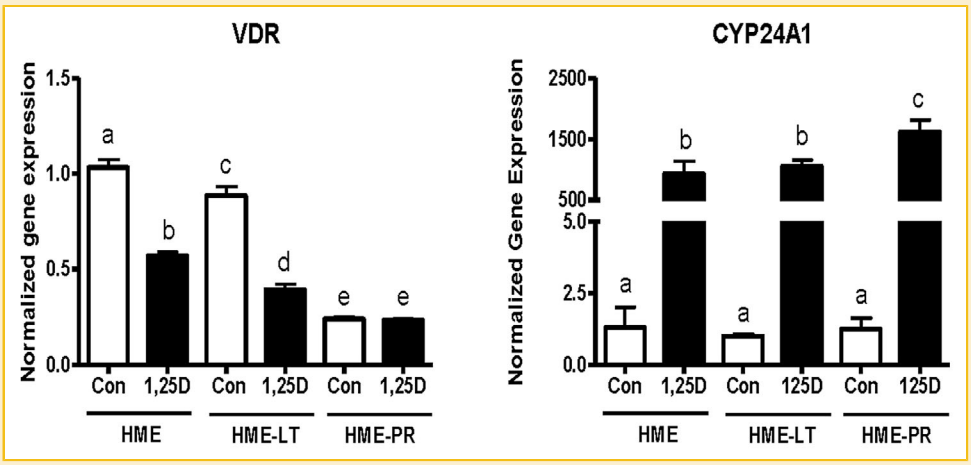

Fig. 3. Quantitative PCR analysis of *VDR* and *CYP24A1* expression in the HME model of mammary cell transformation. HME, HME-LT, and HME-PR cells were treated with 100 nM 1,25D or ethanol vehicle (Con) for 24 h. RNA was isolated and real-time quantitative PCR was conducted for *VDR* and *CYP24A1*. The data were normalized against 18S and expressed relative to values for the vehicle treated HME parental cells. Each bar represents mean ± standard deviation of 3–4 independent samples analyzed in duplicate. *Bars annotated with different letters are significantly different (*P*-value <0.05) as assessed by one-way ANOVA. Two-way ANOVA indicated a significant interaction between cell line and treatment for both VDR and CYP24A1.

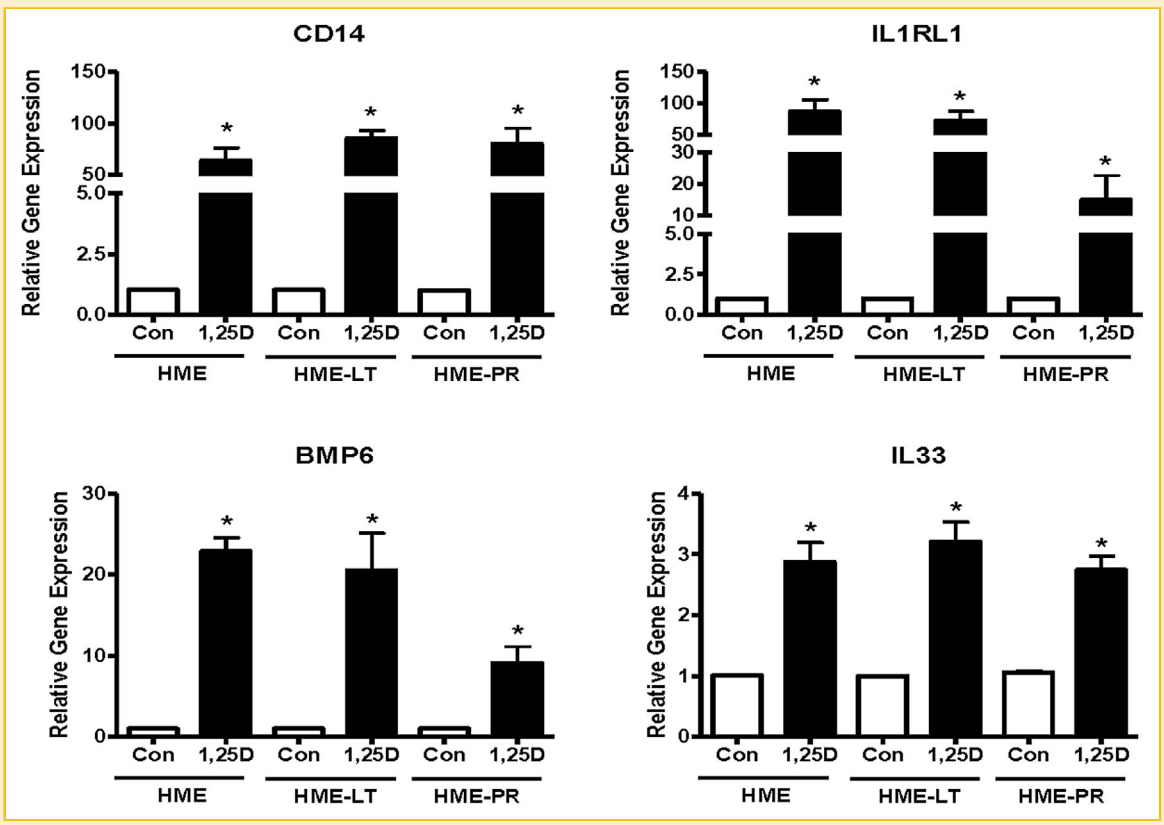

Fig. 4. Effect of 1,25D on expression of *CD14*, *IL1RL1*, *BMP6*, and *IL33* in HME cells and transformed derivatives. HME, HME-LT and HME-PR cells were treated with 100 nM 1,25D or ethanol vehicle (Con) for 24 h. RNA was isolated and real-time quantitative PCR was conducted for *CD14*, *IL1RL1*, *BMP6*, and *IL33*. The data were normalized against 18S and 1,25D treated values were expressed relative to vehicle treated values within each cell line. Each bar represents mean ± standard deviation of at least three independent samples analyzed in duplicate. *P-value <0.05 for the effect of 1,25D within each cell line as assessed by unpaired t-test. Two-way ANOVA indicated a significant interaction between cell line and treatment for the *IL1RL1* and *BMP6* genes.

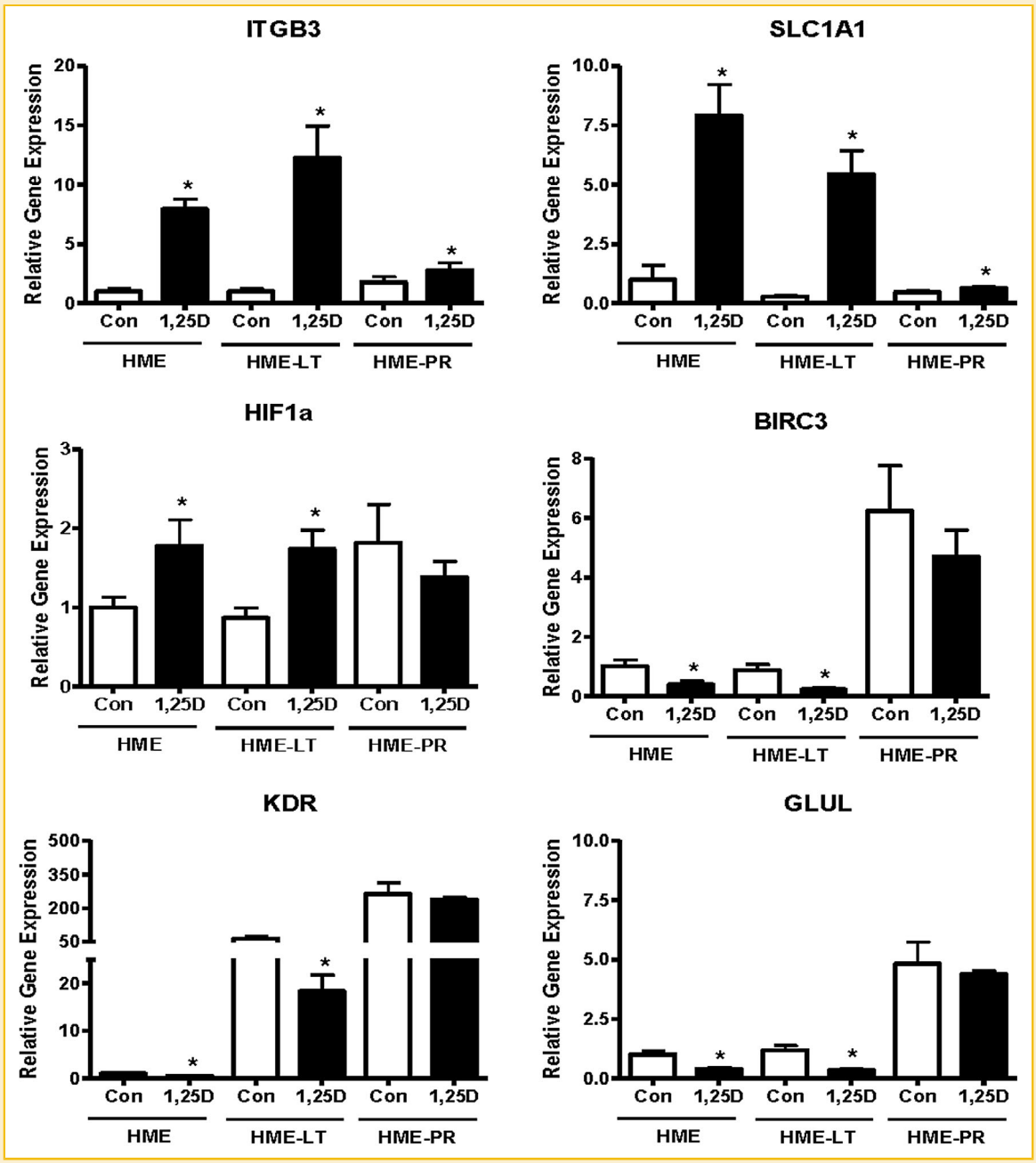

Fig. 5. Effect of 1,25D on expression of genes related to cellular metabolism and hypoxia in HME cells and transformed derivatives. HME, HME-LT and HME-PR cells were treated with 100 nM 1,25D or ethanol vehicle (Con) for 24 h. RNA was isolated and real-time quantitative PCR was conducted for *ITGB3*, *SLC1A1*, *HIFA*, *BIRC3*, *KDR* and *GLUL*. The data were normalized against 18S and 1,25D treated values were expressed relative to vehicle treated values within each cell line. Each bar represents mean ± standard deviation of at least three independent samples analyzed in duplicate. *P-value <0.05 for the effect of 1,25D within each cell line as assessed by unpaired t-test. Two-way ANOVA indicated a significant interaction between cell line and treatment for the *ITGB3* and *SLC1A1* genes.

We used PCR to directly compare the effects of 1,25D on expression of eight highly regulated genes from the MCF7 dataset in both MCF7 and hTERT-HME cells (Figs. 7, 8). For these analyses we normalized expression of each gene to that of untreated MCF7 cells (which was set to 1.0) in order to assess whether baseline expression altered sensitivity of that gene to 1,25D regulation. Seven (*KLK6*, *TRPV6*, *PMP22*, *IL1R1*, *CLDN1*, *CP*, and *MERTK*) of the eight genes examined were confirmed by PCR to be regulated by 1,25D in MCF7 cells (the exception was *CTGF*). Interestingly, four of these genes (*KLK6*, *TRPV6*, *PMP22*, and *IL1R1*) were found to be similarly regulated in hTERT-HME cells by PCR although they were not identified in the hTERT-HME array dataset. The remaining four genes (*CLDN1*, *CP*, *MERTK*, and *CTGF*) were not similarly regulated between the two cell types. Two-way ANOVA indicated significant

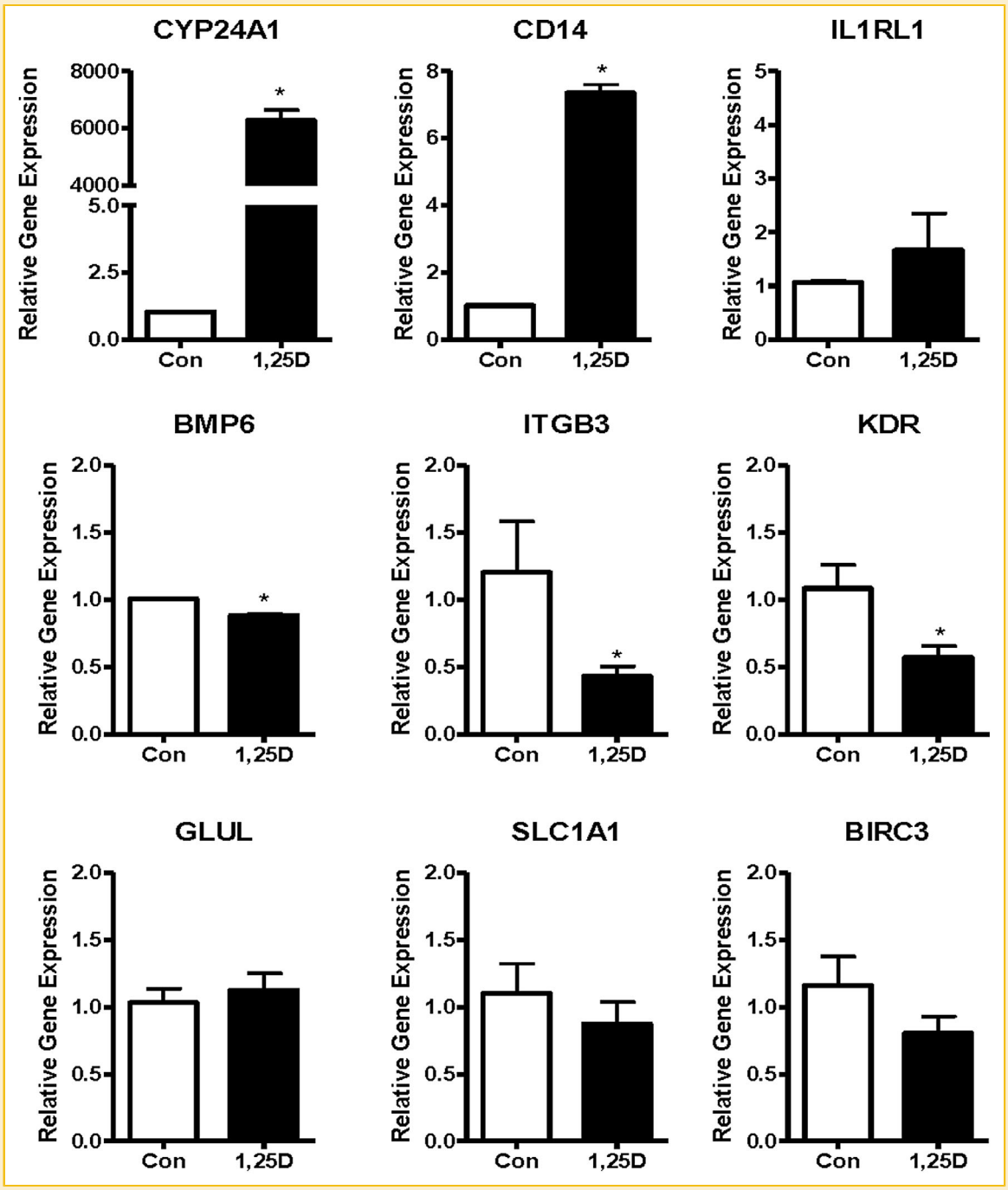

Fig. 6. Effect of 1,25D on expression of *CYP24A1*, *CD14*, *IL1RL1*, *BMP6*, *ITGB3*, *KDR*, *GLUL*, *SLC1A1*, and *BIRC3* in MCF7 cells. MCF7 cells were treated with 100 nM 1,25D or ethanol vehicle (Con) for 24 h. RNA was isolated and real-time quantitative PCR was conducted for *CYP24A1*, *CD14*, *IL1RL1*, *BMP6*, *ITGB3*, *KDR*, *GLUL*, *SLC1A1*, and *BIRC3*. The data were normalized against 18S and expressed relative to control values which were set to 1. Each bar represents mean ± standard deviation of three independent samples analyzed in duplicate. *P-value <0.05 1,25D vs. control as assessed by one-tailed, unpaired t-test.

differences in 1,25D responsiveness between hTERT-HME and MCF7 cells for several genes: induction of *KLK6*, *TRPV6*, and *CTGF* was significantly greater in hTERT-HME cells whereas induction of *CP* and *MERTK* and down-regulation of *CLDN1* were significantly greater in MCF7 cells. Some of the differences in gene regulation by 1,25D may be related to differences in baseline expression, which were noted for *CLDN1* and *CTGF*. For example, basal expression of CLDN1 was high in MCF7 cells (where it was down-regulated by 1,25D), but very low in hTERT-HME cells (which may have precluded further down-regulation upon 1,25D treatment). Conversely, the baseline expression of *CTGF* was low in MCF7 cells and the down-regulation by 1,25D identified on the array dataset was not

TABLE VI. Top 20 Up-Regulated Genes in MCF7 Cells Exposed to 100 nM 1,25D for 24 h

Gene symbol	Gene description	Fold change[1]	Corrected *P*-value[2]
CYP24A1	Cytochrome P450 Family 24A1	277.37	7.03E-08
KLK6	Kallikrein-Related Peptidase 6	10.42	2.05E-05
CP	Ceruloplasmin	8.28	1.44E-05
TRPV6	Transient Receptor Potential Cation Channel V6	6.74	3.97E-05
MERTK	C-Mer Proto-Oncogene Tyrosine Kinase	3.82	3.97E-05
CAMP	Cathelicidin Antimicrobial Peptide	3.63	8.98E-05
CLMN	Calmin	3.30	3.97E-05
IGFBP5	Insulin-Like Growth Factor Binding Protein 5	3.27	5.28E-05
CYP1A1	Cytochrome P450 Family 1 Subfamily A Polypeptide 1	3.20	3.97E-05
TIMP3	TIMP Metallopeptidase Inhibitor 3	3.09	3.97E-05
PRKG2	Protein Kinase cGMP-Dependent Type II	3.07	5.15E-05
ITPR1	Inositol 1,4,5 5-Triphosphate Receptor Type 1	2.77	6.73E-05
DCLK1	Doublecortin-like Kinase 1	2.74	1.74E-04
FSTL4	Follistatin-Like 4	2.71	1.43E-04
AREG	Amphiregulin	2.70	5.03E-05
TRANK1	Tetratricopeptide Repeat Ankyrin Repeat Containing 1	2.61	2.38E-04
PGM2L1	Phosphoglucomutase 2-Like 1	2.50	2.39E-04
ITGA2	Integrin Alpha 2	2.46	9.88E-05
IGFBP3	Insulin-like Growth Factor Binding Protein 3	2.41	7.85E-04
ARHGEF6	Rac/Cdc42 Guanine nucleotide Exchange Factor 6	2.35	7.27E-05

[1]Fold change in MCF7 cells treated with 100nM 1,25D relative to ethanol vehicle was calculated from microarray data with Gene Spring.
[2]*P*-values were generated by moderated *t*-test with Benjamini Hochberg correction.

confirmed, however in hTERT-HME cells baseline *CTGF* expression was high and significant down-regulation was observed upon 1,25D treatment.

To identify common genes and pathways altered by VDR activation, we used Venn analysis and WIKI pathways to compare the datasets generated in the two cell lines. A Venn diagram using a fold change cutoff of 1.5 (483 entities for hTERT-HME cells and 249 entities for MCF7 cells) identified 32 overlapping entities (Fig. 9). Of these, 26 entities corresponding to 21 annotated genes (17 up-regulated and 4 down-regulated) were modulated in the same direction in both cell lines (Table IX). The remaining overlapping entities were altered in both cell lines but in opposite directions (Supplementary Table S7). Of the 21 commonly regulated annotated genes, only two (*CYP24A1* and *CAMP)* were on the top 20 list for both cell lines.

COMPARATIVE ANALYSIS WITH PUBLICALLY AVAILABLE GENOMIC PROFILES

To further interrogate 1,25D gene signatures in models of breast cancer, we searched the literature for additional reports on VDR target genes in breast cells. Although several papers contain partial reports of array screening with 1,25D or synthetic analogs in breast cells using a variety of platforms and protocols [Swami et al., 2003; Lee et al., 2006; Vanoirbeek et al., 2009], we identified only two publically available microarray datasets of 1,25D treatment in breast model systems for comparison to our data. Goeman et al. [Goeman et al., 2014] utilized RNA–SEQ to generate a list of differentially expressed genes in SKBR3 cells (a model of HER2 positive breast cancer with mutant p53) treated for 6 h with 100 nM 1,25D. Comparison of this dataset with our data from hTERT-HME and MCF7 cells identified 17 genes that were altered by 1,25D exposure

TABLE VII. Top 20 Down-Regulated Genes in MCF7 Cells Exposed to 100 nM 1,25D for 24 h

Gene symbol	Gene description	Fold change[1]	Corrected *P*-value[2]
PMP22	Peripheral Myelin Protein 22	−3.26	9.88E-05
CTGF	Connective Tissue Growth Factor	−2.76	3.12E-04
CLDN1	Claudin 1	−2.13	1.74E-04
IL1R1	Interleukin 1 Receptor Type 1	−2.10	1.97E-04
UGT2B7	UDP Glucuronosyltransferase 2 Family B7	−1.86	2.09E-02
LUZP2	Leucine Zipper Protein 2	−1.84	2.53E-04
COL12A1	Collagen Type XII Alpha 1	−1.84	1.97E-04
EHF	ETS Homologous Factor	−1.79	6.33E-04
ANXA1	Annexin A1	−1.78	8.99E-04
ANKRD30B	Ankyrin Repeat Domain 3 OB	−1.77	4.73E-04
RNF144B	Ring Finger Protein 144B	−1.77	3.43E-04
RGS2	Regulator of G-Protein Signaling 2	−1.75	2.39E-04
CAV1	Caveolin 1	−1.75	2.11E-04
EGLN3	EGL Nine Homolog 3	−1.74	2.39E-04
RAB27B	RAS Oncogene Family Member	−1.71	5.96E-04
SLC25A30	Solute Carrier Family 25 Member 30	−1.70	1.29E-03
KCNJ8	Potassium Inwardly-Rectifying Channel J8	−1.68	2.44E-03
KLF6	Kruppel-like factor 6	−1.68	4.60E-04
SON	Scinderin	−1.67	3.43E-04
TSPAN12	Tetraspanin 12	−1.67	3.43E-04

[1]Fold change in MCF7 cells treated with 100nM 1,25D relative to ethanol vehicle was calculated from microarray data with Gene Spring.
[2]*P*-values were generated by moderated *t*-test with Benjamini Hochberg correction.

TABLE VIII. Pathway Analysis of Genes Differentially Expressed in MCF7 Cells Exposed to 100 nM 1,25D for 24 h

Pathway	*P*-value[1]	Matched entities[2]	Number of pathway entities[3]
Phase 1 Functionalization of Compounds	6.31E-04	4	49
Oncostatin M Signaling Pathway	1.90E-03	4	65
Myometrial Relaxation and Contraction Pathways	1.94E-03	6	156
Regulation of Insulin-like Growth Factor (IGF) Activity by Insulin-like Growth Factor Binding Proteins (IGFBPs)	2.98E-03	2	10
Tryptophan metabolism	6.65E-03	3	80
Integrin-mediated Cell Adhesion	9.53E-03	4	99
Senescence and Autophagy	9.53E-03	4	106
TGF-Beta Signaling Pathway	1.04E-02	3	55
ATM Signaling Pathway	1.56E-02	2	41
Endochondral Ossification	1.64E-02	3	64
Quercetin and NF-kB-AP-1 induced cell apoptosis	1.66E-02	1	15
Adipogenesis	2.36E-02	4	131
B-Cell Receptor	2.73E-02	4	136
Prostaglandin Synthesis and Regulation	2.74E-02	2	31
Ovarian Infertility Genes	2.91E-02	2	32
Apoptosis Modulation and Signaling	2.93E-02	3	93
Brain-derived Neurotrophic Factor Signaling Pathway	2.99E-02	4	141
Nuclear Receptors in Lipid Metabolism and Toxicity	3.08E-02	2	35
Cell surface interactions at the vascular wall	3.26E-02	2	39
Tamoxifen metabolism	3.29E-02	1	21
Estrogen metabolism	3.29E-02	1	18
T-Cell Receptor Signaling Pathway	3.95E-02	3	92
Diclofenac Metabolic Pathway	4.10E-02	1	5
Effects of Nitric Oxide	4.10E-02	1	8
Vitamin A and Carotenoid Metabolism	4.19E-02	2	43
Interleukin-11 Signaling Pathway	4.39E-02	2	40
Integrated Pancreatic Cancer Pathway	4.39E-02	2	200
Androgen Receptor	4.40E-02	3	94
Nicotine Metabolism	4.90E-02	1	6
Fanconi Anemia pathway	4.90E-02	1	6

[1]*P*-values were calculated for pathway enrichment with Wiki Pathway Beta.
[2]Number of matched entities from the microarray dataset.
[3]Total number of entities for each pathway.

in all three breast-derived cell lines, however, only 11 of these genes were regulated in the same direction (9 up, 2 down) after 1,25D treatment (Table IX). Additional comparisons identified 26 genes (24 up, 2 down) commonly regulated by 1,25D in both cancer cell lines (SKBR3 and MCF7 cells) and 20 genes (14 up, 6 down) commonly regulated by 1,25D in both SKBR3 and hTERT-HME cells. The specific genes in each list are detailed in Table X. A caveat to these comparisons is that the shorter duration of treatment (6 h) in Goerman's study compared to ours (24 h) would underestimate the number of overlapping targets. Genes identified after a 24 h treatment period will include both primary VDR target genes and downstream effectors (i.e., secondary targets), and it might be anticipated that alterations in these secondary targets would be more variable in different model systems. On the other hand, many of the genes that were commonly altered in our analysis (*CLMN*, *CD97*, *CD14*, *SERPINB1*, *IGFBP3*) were also identified in a screen of transformed breast cells treated with the synthetic 1,25D analog Ro3582 [Lee et al., 2006].

Finally we used the genomic dataset of Milani et al. [Milani et al., 2013] which represents differentially expressed genes in heterogeneous human breast tumor explants exposed to 1,25D (100 nM, 24 h) ex vivo to identify the subset of genes regulated by 1,25D in established cell lines that was also regulated in intact tissue (Table X). This comparison identified four genes (*CYP24A1, CLMN, EFTUD1,* and *SERPINB1*) that were up-regulated by 1,25D in the tumor explants and in all three breast-derived cell lines. A fifth gene, *IL1RL1*, was common to all four datasets but was down-regulated in SKBR3 cells and up-regulated in the other three model systems. There were no genes identified that were down-regulated by 1,25D in all model systems.

DISCUSSION

VDR agonists such as 1,25D and synthetic vitamin D analogs exert profound effects on cancer cell behavior and dozens of VDR regulated genes, proteins and pathways have been identified in various model systems of cancer [Fleet et al., 2012]. In addition, evidence suggests that VDR signaling in normal epithelial cells exerts tumor suppressor actions that contribute to cancer prevention. Despite the known molecular action of the liganded VDR as a transcription factor, the comprehensive genomic signatures associated with 1,25D exposure in normal and cancer cells have not been extensively studied. Although most tumor cell lines and biopsied human cancers retain expression of VDR, several studies have suggested that vitamin D metabolism and/or VDR signaling becomes deregulated during cancer progression. In these studies we have addressed these research gaps by comparative microarray profiling and target gene validation in cells derived from normal and cancerous tissue using models of breast cancer.

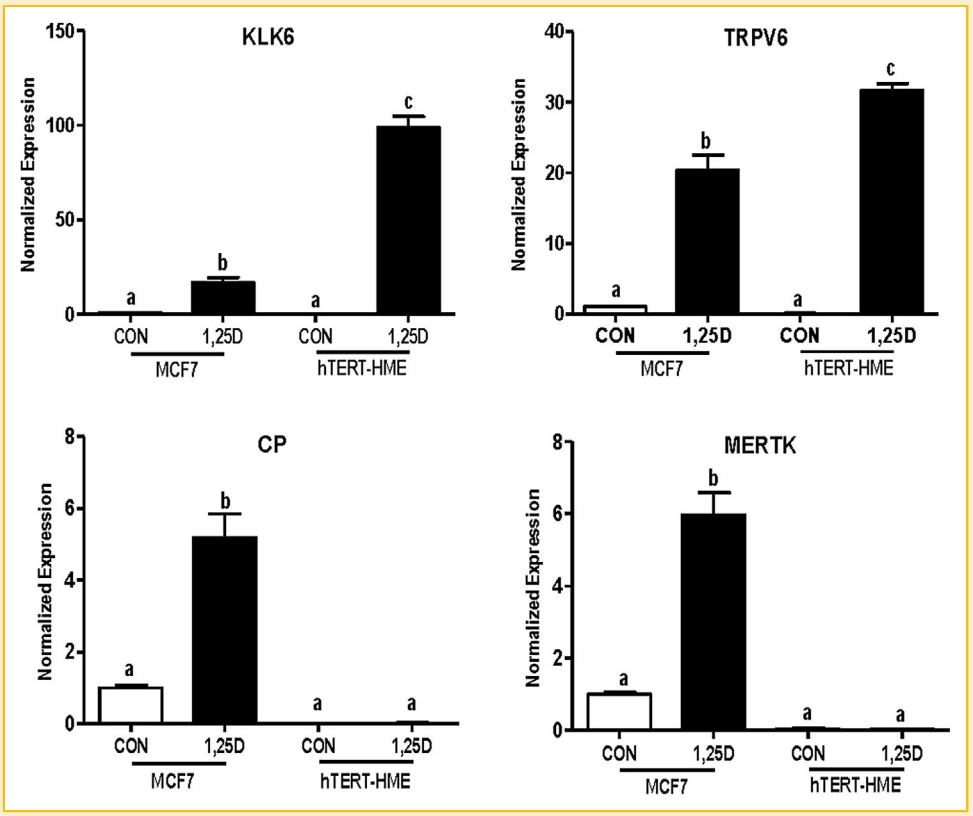

Fig. 7. Comparative effects of 1,25D in MCF7 and hTERT-HME cells on up-regulated genes identified as potential VDR targets by microarray analysis of 1,25D treated MCF7 cells. MCF7 and hTERT-HME cells were treated with 100 nM 1,25D or ethanol vehicle (Con) for 24 h. RNA was isolated and real-time quantitative PCR was conducted for *KLK6, TRPV6, CP,* and *MERTK*. The data were normalized against 18S and expressed relative to values for control treated MCF7 cells which were set to 1. Each bar represents mean ± standard deviation of three independent samples analyzed in duplicate. *Bars annotated with different letters are significantly different (*P*-value <0.05) as assessed by one-way ANOVA. Two-way ANOVA indicated a significant interaction between cell line and treatment for all genes.

This is the first report to comprehensively annotate the genomic signature of 1,25D exposure in cells derived from normal mammary tissue (hTERT-HME cells). In previous studies, we demonstrated that hTERT-HME cells express VDR and exhibit biological responses similar to primary cultures of human breast epithelial cells when treated with 1,25D [Kemmis et al., 2006]. The genomic datasets reported here support the concept that 1,25D mediates anti-cancer signaling in these cells and identify multiple novel VDR targets. Within 24 h of treatment, 1,25D treatment enriched for genes in major tumor suppressive pathways (i.e., cell adhesion, senescence, Nrf2 signaling), immune responses (cytokines, toll-like receptor signaling) and cellular energy metabolism (pentose pathway, lipid metabolism, leptin signaling) in hTERT-HME cells. A cohort of 11 immune response genes (including *CD14*, *IL1RL1*, *TREM1,* and *TLR4*) were verified as 1,25D responsive in these cells. Many of these genes (i.e., *CD14*, *TLR4*, *CAMP*) are well recognized as VDR targets in immune cells and have also been reported as 1,25D responsive in epithelial cells [Fleet et al., 2012]. *CD14*, the second most highly up-regulated gene in the hTERT-HME dataset, is particularly interesting in the context of normal mammary gland biology as it has been implicated in breast progenitor cell self-renewal, tissue remodeling during involution and protection against mastitis [Vidal and Donnet-Hughes, 2008; Wall et al., 2009; Scheeren et al., 2014]. Soluble CD14 is also secreted from mammary epithelial cells into breast milk where it likely impacts neonatal immunity [Zheng et al., 2006]. These observations warrant follow-up studies to determine whether vitamin D status alters the expression or function of *CD14* or other immune response genes in mammary tissue in vivo. An additional set of seven genes involved in cellular metabolism and hypoxia (including *GLUL*, *SLC1A1*, *HIF1A,* and *KDR*) were verified as VDR targets in the hTERT-HME cells. Although for the most part these genes have not been well studied in the context of breast cancer, they function in pathways predicted to be relevant to cancer prevention. *GLUL* (which encodes glutamine synthase) is an essential mediator of mammary epithelial cell survival during glutamine deprivation [Kung et al., 2011]. *SLC1A1* encodes a membrane glutamate transporter which contributes to protection against oxidative stress via enhancing glutathione synthesis [Aoyama et al., 2006]. *HIF1A* is a critical sensor of oxygen availability and angiogenesis whereas *KDR* encodes the major receptor for VEGF and regulates breast cancer cell apoptosis [Zhang et al., 2014]. These data implicate 1,25D in control of glutamine metabolism, anti-oxidant signaling and hypoxia, important mediators of the metabolic switch associated with cancer progression [Bensaad and Harris, 2014].

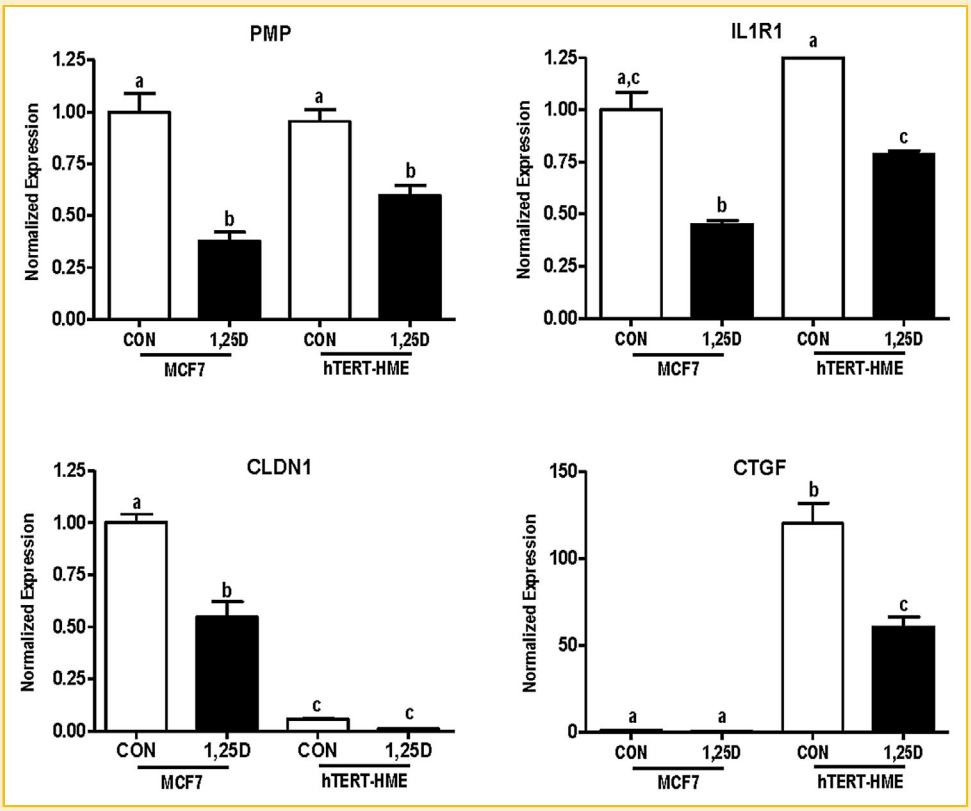

Fig. 8. Comparative effects of 1,25D in MCF7 and hTERT-HME cells on down-regulated genes identified as potential VDR targets by microarray analysis of 1,25D treated MCF7 cells. MCF7 and hTERT-HME cells were treated with 100 nM 1,25D or ethanol vehicle (Con) for 24 h. RNA was isolated and real-time quantitative PCR was conducted for *PMP22, IL1R1, CLDN1,* and *CTGF*. The data were normalized against 18S and expressed relative to values for control treated MCF7 cells which were set to 1. Each bar represents mean ± standard deviation of three independent samples analyzed in duplicate. *Bars annotated with different letters are significantly different (*P*-value <0.05) as assessed by one-way ANOVA. Two-way ANOVA indicated a significant interaction between cell line and treatment for the *CLDN1* and *CTGF* genes.

TABLE IX. List of Annotated Genes Commonly Altered by 1,25D in hTERT-HME Mammary Epithelial Cells and MCF7 Breast Cancer Cells

		hTERT HME cells		MCF7 cells	
Gene symbol	Gene description	Fold change[1]	Corrected *P*-value[2]	Fold change[1]	Corrected *P*-value[2]
CYP24A1	Cytochrome P450, Family 24A1	181.37	2.42E-10	277.37	4.32E-08
SERPINB1	Seipin Peptidase Inhibitor, Clade B, Member 1	4.32	2.45E-07	2.08	1.27E-04
IGFBP3	Insulin-Like Growth Factor Binding Protein 3	3.79	3.30E-07	2.41	7.85E-04
G6PD	Glucose-6-Phosphate Dehydrogenase	3.73	1.41E-07	1.61	3.76E-04
CD274	CD274 Molecule	3.61	2.61E-06	1.73	1.22E-03
P2RY2	Purinergic Receptor P2 Y, G-Protein Coupled, 2	3.40	6.98E-07	1.62	4.46E-04
EFTUD1	Elongation Factor Tu GTP Binding Domain Containing 1	2.51	1.53E-06	1.95	3.51E-04
CAMP	Cathelicidin Antimicrobial Peptide	2.40	7.78E-06	3.63	5.51E-05
CLMN	Calmin	2.36	8.16E-06	3.30	2.44E-05
VLDLR	Very Low Density Lipoprotein Receptor	2.01	1.45E-05	1.51	4.46E-04
SLC4A7	Solute Carrier Family 4, Sodium Bicarbonate co-transporter, Member 7	1.94	2.33E-05	1.91	1.11E-04
TIMP3	TIMP Metallopeptidase Inhibitor 3	1.93	2.61E-04	3.09	2.44E-05
CD97	CD97 Molecule	1.91	1.85E-05	1.55	3.51E-04
BHLHE40	Basic Helix-Loop-Helix Family, Member E40	1.89	1.42E-05	1.60	3.24E-04
AKR1C3	Aldo-Keto Reductase Family 1, Member C3	1.85	7.81E-06	1.87	4.84E-04
RGNEF	190 kDa Guanine Nucleotide Exchange Factor	1.57	2.10E-04	1.51	4.57E-04
TRPV6	Transient Receptor Potential Cation Channel V6	1.55	1.04E-03	6.74	2.44E-05
RGS2	Regulator of G-protein Signaling 2, 24kDa	−5.01	5.66E-07	−1.75	5.07E-04
CTGF	Connective Tissue Growth Factor	−1.68	6.65E-05	−2.76	5.07E-04
KLF6	Kruppel-like Factor 6	−1.64	7.09E-05	−1.68	6.11E-04
RNF144B	Ring Finger Protein 144B	−1.53	1.52E-04	−1.77	5.07E-04

[1]Fold change in hTERT-HME or MCF7 cells treated with 100 nM 1,25D relative to ethanol vehicle was calculated from microarray data with Gene Spring.
[2]*P*-values were generated by moderated *t*-test with Benjamini Hochberg correction.

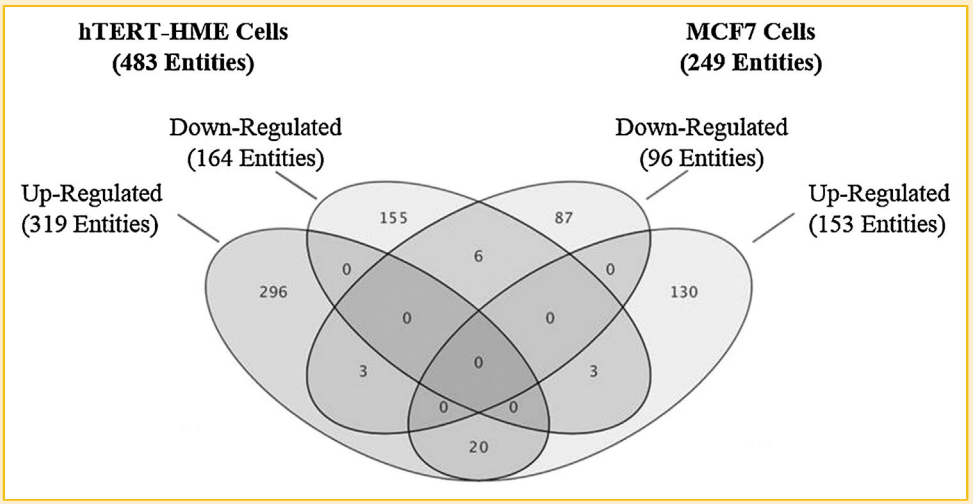

Fig. 9. Venn diagram of 1,25D regulated entities in hTERT-HME and MCF7 cells. hTERT-HME and MCF7 cells were treated for 24 h with 100 nM 1,25D and processed for microarray screening on Gene ST 1.0 arrays. Data were analyzed on Gene Spring v 12.6 software and a Venn diagram was constructed for entities significantly ($P < 0.05$) altered with fold change of >1.5 (483 entities for hTERT-HME cells and 249 entities for MCF7 cells). The 26 entities that were similarly altered by 1,25D in both cell lines corresponded to 21 annotated genes (listed in Table IX).

Collectively, our studies have identified several novel 1,25D responsive genes involved in immune responses and cellular metabolism that are worthy of follow-up in the context of breast cancer.

Our data also clearly demonstrate that the genomic signature of 1,25D exposure in cells derived from normal mammary tissue (hTERT-HME cells) is distinct from that of cells derived from breast cancer (MCF7 cells). Not only was the number of genes altered by 1,25D much higher in hTERT-HME cells than in MCF7 cells (483 vs. 249 respectively), but there was limited overlap between the datasets. Only 21 genes were found to be similarly regulated by 100 nM 1,25D in both model systems. Furthermore, distinct pathways and GO terms were associated with the 1,25D regulated gene lists identified in each cell line. This is not too surprising since the biological effects of 1,25D differ in the two cell lines (MCF7 cells predominantly exhibit growth arrest, autophagy, and apoptosis whereas hTERT-HME cells exhibit growth arrest, adhesion, and changes in metabolism). It is also likely that VDR function becomes altered in cancer cells, as suggested by data reported here demonstrating deregulation of 1,25D mediated gene regulation in normal mammary cells engineered to undergo epithelial-mesenchymal transition (EMT) and supported by the work of others in SKBR3 cells that express mutant p53 [Stambolsky et al., 2010]. Furthermore, it is clear that the genomic rearrangements, mutations, and epigenetic alterations that are characteristic of cancer cells modify both baseline gene expression and transcriptional regulation which could substantially alter responses to 1,25D. For example, some of the genes that are up-regulated by 1,25D in normal breast epithelial cells but not in MCF7 cells (i.e., *SLC1A1*, *ITGB3*) could be epigenetically silenced as a function of carcinogenesis.

The underlying basis for the observed changes in 1,25D mediated gene regulation as a function of EMT requires further study. Oncogenes including constitutively active RAS (used in this study) have been linked to 1,25D resistance via effects on RXR [Solomon et al., 2001; Stedman et al., 2003; Zhang et al., 2010], however, our data indicate that deregulation of VDR signaling by RAS is only partial. Specifically, we show that although the ability of 1,25D to induce and repress many gene targets is blunted and/or abrogated in RAS-transformed cells, *CYP24A1* and several immune response genes examined (such as *CD14*, *IL1RL1*, and *IL33*) remain highly inducible by 1,25D in these cells. This may indicate distinct modes of regulation by 1,25D for these genes, such as the involvement of heterodimer partners other than RXR or in association with post-translational modifications of VDR or RXR [Zhang et al., 2010]. Oncogenic RAS drives kinase signaling and although VDR has several known phosphorylation sites, the specific kinases and phosphatases that regulate VDR phosphorylation and the consequences of this post-translational modification with respect to global gene signatures have not been fully defined [Jurutka et al., 2002; Ting et al., 2012]. However, phosphorylation of other nuclear receptors, notably PPARγ, has been shown to selectively alter gene signatures in a disease-relevant manner [Choi et al., 2010]. Further study will be required to explore these possibilities.

In contrast to the effects observed in cells expressing the RAS oncogene, we found little evidence that 1,25D-mediated gene expression is altered in hTERT-HME cells expressing SV40-derived oncogenic sequences which disable p53 signaling. This observation is consistent with early studies that demonstrated that breast cancer cells expressing mutant forms of p53 (such as T47D) retain sensitivity to 1,25D-mediated growth arrest [Eisman et al., 1987]. However, as noted above, studies in SKBR3 breast cancer cells suggest that certain p53 mutant proteins can complex with VDR and substantially alter 1,25D mediated gene regulation including some of the targets identified in our models such as KLK6 [Stambolsky et al., 2010]. We therefore compared the datasets generated in hTERT-HME and MCF7 cells (which express wild-type p53) to that of

TABLE X. Gene Signatures[1] of 1,25D Exposure in Mammary-Derived Cell Lines (hTERT-HME, MCF7, SKBR3) and in Breast Tumor Explants

Genes common to all 3 cell lines	Genes common to MCF7 and SKBR3	Genes common to hTERT-HME and SKBR3	Genes common to all 4 datasets
CLMN (↑)	CLMN (↑)	CLMN (↑)	CLMN (↑)
CYP24A1 (↑)	CYP24A1 (↑)	CYP24A1 (↑)	CYP24A1 (↑)
EFTUD1 (↑)	EFTUD1 (↑)	EFTUD1 (↑)	EFTUD1 (↑)
IL1RL1	IL1RL1	IL1RL1 (↑)	IL1RL1
SERPINB1 (↑)	SERPINB1 (↑)	SERPINB1 (↑)	SERPINB1 (↑)
BHLHE40	BHLHE40	BHLHE40	
CD97 (↑)	CD97 (↑)	CD97 (↑)	
ETS2	ETS2	ETS2	
G6PD	G6PD	G6PD	
IGFBP3	IGFBP3	IGFBP3	
NDRG1 (↓)	NDRG1 (↓)	NDRG1 (↓)	
RGNEF (↑)	RGNEF (↑)	RGNEF (↑)	
SDC3 (↓)	SDC3 (↓)	SDC3 (↓)	
SLC26A2	SLC26A2	SLC26A2	
TIMP3 (↑)	TIMP3 (↑)	TIMP3 (↑)	
TRPV6 (↑)	TRPY6 (↑)	TRPV6 (↑)	
VLDLR	VLDLR	VLDLR	
	ACOX3	ARSJ (↓)	
	AREG (↑)	BDKRB1 (↑)	
	ARHGEF6	DNAJB1	
	CDK6 (↓)	DUSP1	
	CEACAM6 (↑)	EFNA1 (↓)	
	CEBPB (↑)	EFNB2 (↓)	
	CYP1A1 (↑)	GRK5	
	DHRS3	HR	
	FAM46C	KLF14	
	ITPR1 (↑)	KRT16 (↑)	
	MB	MALL	
	MERTK (↑)	RASD2 (↑)	
	NFKBIA	RASSF5	
	PADI3 (↑)	RIPK4	
	PGM2L1 (↑)	SEMA3B (↑)	
	PHLDB2 (↑)	SERPINB6	
	PISD (↑)	SRGAP3 (↓)	
	SMOX (↑)	TMEM40	
	STEAP4 (↑)	TTC7A (↑)	
	SULT2B1		
	TGIF1		
	TMPRSS2 (↑)		
	TSKU (↑)		
	ZNF703 (↑)		

[1]Gene signatures were compiled as described in Methods by integrating the hTERT-HME and MCF7 datasets reported here with those of Goerman et al. (22) and Milani et al. (26).

SKBR3 cells (which express mutant p53) and identified distinct cohorts of genes (including *IL1RL1*, *BHLHE40*, *ETS2,* and *IGFBP3*) that were oppositely regulated by 1,25D treatment in each cell line. Since as noted above the treatment duration for these studies varied, further analysis of the kinetics of gene expression may be informative in resolving these differences. Alternatively, the discrepancies may be related to the genomic context in which p53 deregulation occurs (i.e., non-transformed mammary cells such as hTERT-HME vs. established breast cancer cells such as MCF7, T47D, and SKBR3) and/or the specific p53 alteration expressed in a given cell or tumor. In any case, it is clear that the interactions between VDR and p53 are complex, and are likely to be further confounded in tumor cells exposed to stress or DNA damaging agents. Thus, further studies are warranted to clarify the effects of p53 mutation or loss on 1,25D/VDR signaling in breast cancer.

Despite the different gene profiles associated with 1,25D exposure in each breast-derived cell line, a core signature of 11 1,25D-responsive genes (9 up-regulated and 2 down-regulated) was identified in all three established breast-derived cell lines. More extensive overlap was found between the two breast cancer cell lines (24 up-regulated genes and 2 down-regulated genes), however, as noted earlier this list is likely an underestimate due to differences in 1,25D treatment duration.

We also compared the gene lists from the established breast cell lines to a publically available dataset derived from human breast tumor explants treated for 24 h with 100 nM 1,25D (a model which more accurately represents intact tumor tissue). In addition to *CYP24A1*, this analysis identified four 1,25D-modulated genes (*CLMN*, *EFTUD1*, *IL1RL1,* and *SERPINB1*) that may represent useful biomarkers of vitamin D action for future translational studies. Three of these genes were coordinately regulated by 1,25D in all gene lists examined and are known to function in cancer-relevant pathways: *CLMN* mediates cell-cycle arrest in response to retinoids [Marzinke and Clagett-Dame, 2012], *SERPINB1* inhibits proteases and reduces tissue inflammation [Gong et al., 2011; Huasong et al., 2014] and *EFTUD1* functions in ribosome biogenesis [Finch et al., 2011]. Although these genes have not been extensively studied in breast cancer, loss of expression of *SERPINB1* is correlated with poor survival in hepatocellular carcinoma and loss of *EFTUD1* function is associated with predisposition to leukemia [Finch et al., 2011;

Burwick et al., 2012]. Thus, follow-up to determine the effects of 1,25D on the functions of the proteins encoded by these genes in the context of normal mammary gland and breast cancer is clearly warranted.

In summary, while *CYP24A1* is commonly identified in microarray studies as the most highly up-regulated gene in 1,25D treated cells, other modulated genes vary greatly depending on the model system. While not wholly unexpected as transcriptional responses across cell types is in general highly diverse, determining the molecular basis for these differences is warranted. The distinct biological effects of 1,25D in different cell types could reflect differences in expression of VDR, its RXR partners or transcriptional co-regulators as well as the underlying epigenetic states in specific genomic regions. In addition, adaptation of cells to 2-D culture, use of long-established cell lines and the presence of cancer-associated genomic alterations likely contribute to this diversity. It is worth noting that several of the genes we identified as 1,25D modulated in hTERT-HME cells, including *CD14*, *CD97*, *THBD*, *NINJ1*, *CAMP* and *IL8*, have been identified as direct VDR targets by ChIP-seq and were altered in peripheral blood mononuclear cells by oral vitamin D supplementation, but only in a subset of trial participants [Saksa et al., 2014]. This supports the feasibility of identifying biomarkers of vitamin D exposure through cell culture studies, but also confirms the heterogeneity of individual responses. Continued integration of the datasets reported here with additional genomic profiles and ChIP-Seq data will assist in identifying more comprehensive common and tissue/cell-specific signatures of 1,25D-VDR signaling. The continued use of complex models such as tumor explants for vitamin D studies is desirable given the expression of VDR in most cell types and the critical interactions between tumor cells and their stromal microenvironment.

ACKNOWLEDGEMENTS

The authors would like to acknowledge and thank the following individuals for their technical assistance in conducting and/or analyzing the microarray experiments: Dr. Sridar Chittur (Center for Functional Genomics, University at Albany), Dr. Cintia Milani (São Paulo University, Brazil), Dr. Lei Li (Department of Biomedical Sciences, University at Albany) and Dr. Ana Maria Marchionatti (Universidad Nacional de Córdoba, Argentina).

REFERENCES

Aoyama K, Suh SW, Hamby AM, Liu J, Chan WY, Chen Y, Swanson RA. 2006. Neuronal glutathione deficiency and age-dependent neurodegeneration in the EAAC1 deficient mouse. Nat Neurosci 9:119–126.

Beaudin SG, Robilotto S, Welsh J. 2014. Comparative regulation of gene expression by 1,25-dihydroxyvitamin D in cells derived from normal mammary tissue and breast cancer. J Steroid Biochem Mol Biol Sep 18. pii: S0960-0760(14) 00213–1 Sep 18. pii: S0960-0760(14) 00213–1. doi: 10.1016/j.jsbmb.2014.09.014. [Epub ahead of print] .

Bensaad K, Harris AL. 2014. Hypoxia and metabolism in cancer. Adv Exp Med Biol 772:1–39.

Berger U, Wilson P, McClelland RA, Colston K, Haussler MR, Pike JW, Coombes RC. 1987. Immunocytochemical detection of 1,25-dihydroxyvitamin D3 receptor in breast cancer. Cancer Res 47:6793–6799.

Buras RR, Schumaker LM, Davoodi F, Brenner RV, Shabahang M, Nauta RJ, Evans SR. 1994. Vitamin D receptors in breast cancer cells. Breast Cancer Res Treat 31:191–202.

Burwick N, Coats SA, Nakamura T, Shimamura A. 2012. Impaired ribosomal subunit association in Shwachman-Diamond syndrome. Blood 120:5143–5152.

Byrne B, Welsh J. 2007. Identification of novel mediators of Vitamin D signaling and 1,25(OH) 2D3 resistance in mammary cells. J Steroid Biochem Mol Biol 103:703–707.

Choi JH, Banks AS, Estall JL, Kajimura S, Bostrom P, Laznik D, Ruas JL, Chalmers MJ, Kamenecka TM, Bluher M, Griffin PR, Spiegelman BM. 2010. Anti-diabetic drugs inhibit obesity-linked phosphorylation of PPARgamma by Cdk5. Nature 466:451–456.

Ding N, Yu RT, Subramaniam N, Sherman MH, Wilson C, Rao R, Leblanc M, Coulter S, He M, Scott C, Lau SL, Atkins AR, Barish GD, Gunton JE, Liddle C, Downes M, Evans RM. 2013. A vitamin D receptor/SMAD genomic circuit gates hepatic fibrotic response. Cell 153:601–613.

Eisman JA, Sutherland RL, McMenemy ML, Fragonas JC, Musgrove EA, Pang GY. 1987. Effects of 1,25dihdyroxyvitamin D_3 on cell cycle kinetics of T47D human breast cancer cells. J Cell Physiol 138:611–616.

Elenbaas B, Spirio L, Koerner F, Fleming MD, Zimonjic DB, Donaher JL, Popescu NC, Hahn WC, Weinberg RA. 2001. Human breast cancer cells generated by oncogenic transformation of primary mammary epithelial cells. Genes Dev 15:50–65.

Finch AJ, Hilcenko C, Basse N, Drynan LF, Goyenechea B, Menne TF, Gonzalez Fernandez, D'Santos P, Arends CS, Donadieu MJ, Bellanne-Chantelot J, Costanzo C, Boone M, McKenzie C, Freund AN, Warren SM, . 2011. Uncoupling of GTP hydrolysis from eIF6 release on the ribosome causes Shwachman-Diamond syndrome. Genes Dev 25:917–929.

Fleet JC, DeSmet M, Johnson R, Li Y. 2012. Vitamin D and cancer: A review of molecular mechanisms. Biochem J 441:61–76.

Goeman F, De Nicola F, D'Onorio De Meo P, Pallocca M, Elmi B, Castrignano T, Pesole G, Strano S, Blandino G, Fanciulli M, Muti P. 2014. VDR primary targets by genome-wide transcriptional profiling. J Steroid Biochem Mol Biol 143:348–356.

Gong D, Farley K, White M, Hartshorn KL, Benarafa C, Remold-O'Donnell E. 2011. Critical role of serpinB1 in regulating inflammatory responses in pulmonary influenza infection. J Infect Dis 204:592–600.

Heikkinen S, Vaisanen S, Pehkonen P, Seuter S, Benes V, Carlberg C. 2011. Nuclear hormone 1alpha,25-dihydroxyvitamin D3 elicits a genome-wide shift in the locations of VDR chromatin occupancy. Nucleic Acids Res 39:9181–9193.

Huasong G, Zongmei D, Jianfeng H, Xiaojun Q, Jun G, Sun G, Yan W, Donglin W, Jianhong Z. 2014. Serine protease inhibitor (SERPIN) B1 suppresses cell migration and invasion in glioma cells. Brain Res 1600:59–69.

Jurutka PW, MacDonald PN, Nakajima S, Hsieh JC, Thompson PD, Whitfield GK, Galligan MA, Haussler CA, Haussler MR. 2002. Isolation of baculovirus-expressed human vitamin D receptor: DNA responsive element interactions and phosphorylation of the purified receptor. J Cell Biochem 85:435–457.

Kemmis CM, Salvador SM, Smith KM, Welsh J. 2006. Human mammary epithelial cells express CYP27B1 and are growth inhibited by 25-hydroxyvitamin D-3, the major circulating form of vitamin D-3. J Nutr 136:887–892.

Kemmis CM, Welsh J. 2008. Mammary epithelial cell transformation is associated with deregulation of the vitamin D pathway. J Cell Biochem 105:980–988.

Kim Y, Franke AA, Shvetsov YB, Wilkens LR, Cooney RV, Lurie G, Maskarinec G, Hernandez BY, Le Marchand L, Henderson BE, Kolonel LN, Goodman MT. 2014. Plasma 25-hydroxyvitamin D3 is associated with decreased risk of

postmenopausal breast cancer in whites: A nested case-control study in the multiethnic cohort study. BMC Cancer 14:29.

Kung HN, Marks JR, Chi JT. 2011. Glutamine synthetase is a genetic determinant of cell type-specific glutamine independence in breast epithelia. PLoS Genet 7:e1002229.

Laporta E, Welsh J. (in Press). Modeling vitamin D actions in triple-negative/basal-like breast cancer. J Steroid Biochem Mol Biol. 144(PtA):65–73. doi: 10.1016/j.jsbmb.2013.10.022. Epub 2013 Nov 14 .

Lee HJ, Liu H, Goodman C, Ji Y, Maehr H, Uskokovic M, Notterman D, Reiss M, Suh N. 2006. Gene expression profiling changes induced by a novel Gemini Vitamin D derivative during the progression of breast cancer. Biochem Pharmacol 72:332–343.

Lopes N, Sousa B, Martins D, Gomes M, Vieira D, Veronese LA, Milanezi F, Paredes J, Costa JL, Schmitt F. 2010. Alterations in Vitamin D signalling and metabolic pathways in breast cancer progression: A study of VDR, CYP27B1 and CYP24A1 expression in benign and malignant breast lesions. BMC Cancer 10:483.

Maalmi H, Ordonez-Mena JM, Schottker B, Brenner H. 2014. Serum 25-hydroxyvitamin D levels and survival in colorectal and breast cancer patients: Systematic review and meta-analysis of prospective cohort studies. Eur J Cancer 50(8):1510–1521.doi: 10.1016/j.ejca.2014.02.006. Epub 2014 Feb 28 .

Marzinke MA, Clagett-Dame M. 2012. The all-trans retinoic acid (atRA)-regulated gene Calmin (Clmn) regulates cell cycle exit and neurite outgrowth in murine neuroblastoma (Neuro2a) cells. Exp Cell Res 318:85–93.

Meyer MB, Goetsch PD, Pike JW. 2010. Genome-wide analysis of the VDR/RXR cistrome in osteoblast cells provides new mechanistic insight into the actions of the vitamin D hormone. J Steroid Biochem Mol Biol 121:136–141.

Meyer MB, Goetsch PD, Pike JW. 2012. VDR/RXR and TCF4/β-Catenin cistromes in colonic cells of colorectal tumor origin: Impact on c-FOS and c-MYC gene expression. Mol Endocrinol 26:37–51.

Milani C, Katayama ML, de Lyra EC, Welsh J, Campos LT, Brentani MM, Maciel Mdo, del Valle RA, Goes PR, Nonogaki JC, Tamura S, Folgueira RE, . 2013. Transcriptional effects of 1,25 dihydroxyvitamin D(3) physiological and supra-physiological concentrations in breast cancer organotypic culture. BMC Cancer 13:119.

Mittal MK, Myers JN, Misra S, Bailey CK, Chaudhuri G. 2008. In vivo binding to and functional repression of the VDR gene promoter by SLUG in human breast cells. Biochem Biophys Res Commun 372:30–34.

Mohr SB, Gorham ED, Kim J, Hofflich H, Garland CF. 2014. Meta-analysis of vitamin D sufficiency for improving survival of patients with breast cancer. Anticancer Res 34:1163–1166.

Narvaez CJ, Welsh J. 2001. Role of mitochondria and caspases in vitamin D-mediated apoptosis of MCF-7 breast cancer cells. J Biol Chem 276:9101–9107.

Rowling MJ, Kemmis CM, Taffany DA, Welsh J. 2006. Megalin-mediated endocytosis of vitamin D binding protein correlates with 25-hydroxycholecalciferol actions in human mammary cells. J Nutr 136:2754–2759.

Saksa N, Neme A, Ryynanen J, Uusitupa M, de Mello VD, Voutilainen S, Nurmi T, Virtanen JK, Tuomainen T, Carlberg C. 2014. Dissecting high from low responders in a vitamin D intervention study. J Steroid Biochem Mol Biol 2014 Nov 13. pii: S0960-0760(14) 00267–2. doi: 10.1016/j.jsbmb.2014.11.012. [Epub ahead of print] .

Scheeren FA, Kuo AH, van Weele LJ, Cai S, Glykofridis I, Sikandar SS, Zabala M, Qian D, Lam JS, Johnston D, Volkmer JP, Sahoo D, van de Rijn M, Dirbas FM, Somlo G, Kalisky T, Rothenberg ME, Quake SR, Clarke MF. 2014. A cell-intrinsic role for TLR2-MYD88 in intestinal and breast epithelia and oncogenesis. Nat Cell Biol 16(12):1238–1248.doi: 10.1038/ncb3058. Epub 2014 Nov 2 .

Simboli-Campbell M, Narvaez CJ, Tenniswood M, Welsh J. 1996. 1,25-Dihydroxyvitamin D3 induces morphological and biochemical markers of apoptosis in MCF-7 breast cancer cells. J Steroid Biochem Mol Biol 58:367–376.

Simboli-Campbell M, Narvaez CJ, vanWeelden K, Tenniswood M, Welsh J. 1997. Comparative effects of 1,25(OH) 2D3 and EB1089 on cell cycle kinetics and apoptosis in MCF-7 breast cancer cells. Breast Cancer Res Treat 42:31–41.

So JY, Smolarek AK, Salerno DM, Maehr H, Uskokovic M, Liu F, Suh N. 2013. Targeting CD44-STAT3 signaling by Gemini vitamin D analog leads to inhibition of invasion in basal-like breast cancer. PLoS ONE 8:e54020.

Solomon C, Kremer R, White JH, Rhim JS. 2001. Vitamin D resistance in RAS-transformed keratinocytes: Mechanism and reversal strategies. Radiat Res 155:156–162.

Stambolsky P, Tabach Y, Fontemaggi G, Weisz L, Maor-Aloni R, Siegfried Z, Shiff I, Kogan I, Shay M, Kalo E, Blandino G, Simon I, Oren M, Rotter V. 2010. Modulation of the vitamin D3 response by cancer-associated mutant p53. Cancer Cell 17:273–285.

Stedman L, Nickel KP, Castillo SS, Andrade J, Burgess JR, Teegarden D. 2003. 1,25-Dihydroxyvitamin D inhibits vitamin E succinate-induced apoptosis in C3H10T1/2 Cells but not harvey ras-transfected cells. Nutr Cancer 45:93–100.

Swami S, Raghavachari N, Muller UR, Bao YP, Feldman D. 2003. Vitamin D growth inhibition of breast cancer cells: Gene expression patterns assessed by cDNA microarray. Breast Cancer Res Treat 80:49–62.

Ting HJ, Yasmin-Karim S, Yan SJ, Hsu JW, Lin TH, Zeng W, Messing J, Sheu TJ, Bao BY, Li WX, Messing E, Lee YF. 2012. A positive feedback signaling loop between ATM and the vitamin D receptor is critical for cancer chemoprevention by vitamin D. Cancer Res 72:958–968.

Vanoirbeek E, Eelen G, Verlinden L, Marchal K, Engelen K, De Moor B, Beullens I, Marcelis S, De Clercq P, Bouillon R, Verstuyf A. 2009. Microarray analysis of MCF-7 breast cancer cells treated with 1,25-dihydroxyvitamin D3 or a 17-methyl-D-ring analog. Anticancer Res 29:3585–3590.

Vidal K, Donnet-Hughes A. 2008. CD14: A soluble pattern recognition receptor in milk. Adv Exp Med Biol 606:195–216.

Vrieling A, Seibold P, Johnson TS, Heinz J, Obi N, Kaaks R, Flesch-Janys D, Chang-Claude J. 2014. Circulating 25-hydroxyvitamin D and postmenopausal breast cancer survival: Influence of tumor characteristics and lifestyle factors. Int J Cancer 134(12):2972–2983.doi: 10.1002/ijc.28628. Epub 2013 Dec 7 .

Wall R, Powell A, Sohn E, Foster-Frey J, Bannerman D, Paape M. 2009. Enhanced host immune recognition of mastitis causing Escherchia coli in CD-14 transgenic mice. Anim Biotechnol 20:1–14.

Zhang X, Ge YL, Zhang SP, Yan P, Tian RH. 2014. Downregulation of KDR expression induces apoptosis in breast cancer cells. Cell Mol Biol Lett 19(4):527–541.doi: 10.2478/s11658-014-0210-8. Epub 2014 Sep 2 .

Zhang Z, Kovalenko P, Cui M, Desmet M, Clinton SK, Fleet JC. 2010. Constitutive activation of the mitogen-activated protein kinase pathway impairs vitamin D signaling in human prostate epithelial cells. J Cell Physiol 224:433–442.

Zheng J, Watson AD, Kerr DE. 2006. Genome-wide expression analysis of lipopolysaccharide-induced mastitis in a mouse model. Infect Immun 74:1907–1915.

Zinser GM, McEleney K, Welsh J. 2003. Characterization of mammary tumor cell lines from wild type and vitamin D(3) receptor knockout mice. Mol Cell Endocrinol 200:67–80.

Zinser GM, Welsh J. 2004. Effect of Vitamin D3 receptor ablation on murine mammary gland development and tumorigenesis. J Steroid Biochem Mol Biol 89-90:433–436.

Zugmaier G, Lippman ME. 1990. Effects of TGF beta on normal and malignant mammary epithelium. Ann N Y Acad Sci 593:272–275.

SUPPORTING INFORMATION

Additional supporting information may be found in the online version of this article at the publisher's web-site.